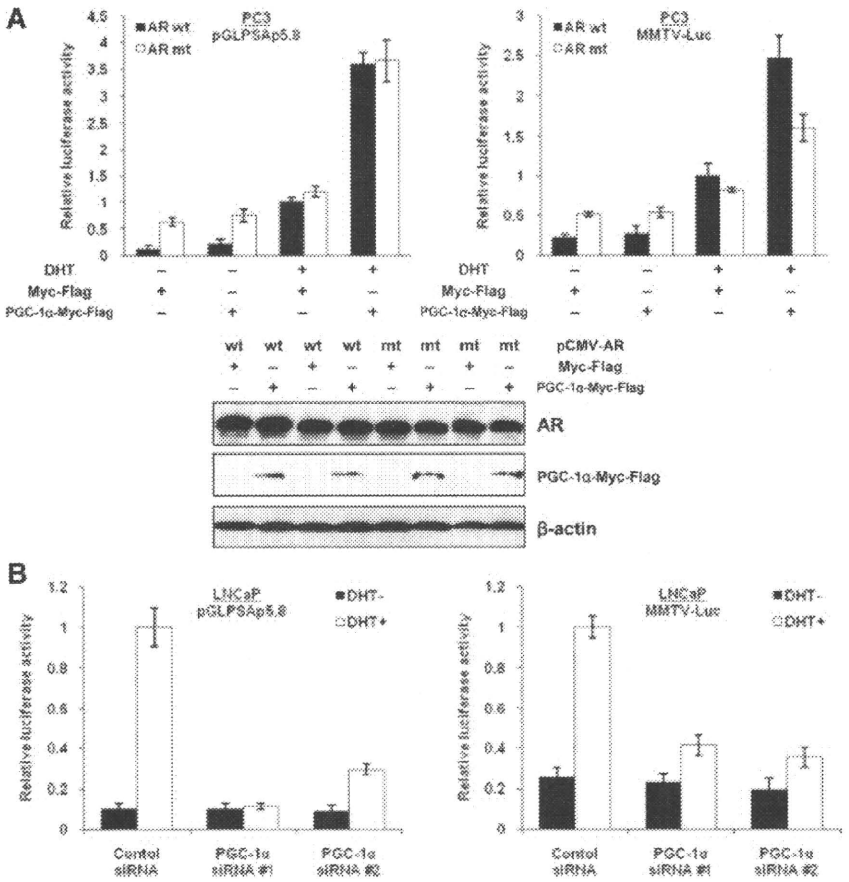

FIG. 3. PGC-1α activates transcriptional activity of AR. A, PC-3 cells were transiently transfected with 0.33 μg of the indicated reporter plasmids, 0.33 μg of Myc-Flag or PGC-1α-Myc-Flag, 0.33 μg of the pCMV-AR [wildtype (wt)] or pCMV-ARmut877 [mutant (mt)], and 0.05 μg of pRL-TK, and incubated in charcoal-stripped medium with or without 10 nM of DHT for 48 h. *Firefly* luciferase activity was corrected for the corresponding *Renilla* luciferase activity. All values represent at least three independent experiments. The luciferase activity of each reporter plasmid with the pCMV-AR and Myc-Flag expression plasmids transfection incubated in charcoal-stripped medium with DHT corresponds to 1. *Boxes*, Mean; *bars*, ± SD. Whole-cell extracts from PC-3 cells transfected with 0.33 μg of each of the indicated plasmids were subjected to SDS-PAGE, and Western blot analysis was performed using anti-Flag, anti-AR (C-19), and anti-β-actin antibodies. B, LNCaP cells were transiently transfected with 20 nM of control siRNA, PGC-1α siRNA no. 1 or PGC-1α siRNA no. 2, followed by transfection with 0.5 μg of the indicated reporter plasmid and 0.05 μg of pRL-TK at intervals of 12 h, and incubated in charcoal-stripped medium with or without 10 nM of DHT. The luciferase assay was performed as described in A. The luciferase activity of each reporter plasmid with control siRNA transfection incubated in charcoal-stripped medium with DHT corresponds to 1. *Boxes*, mean; *bars*, ± SD.

the TAD of AR and was involved in the interaction between the TAD and the LBD of AR, we investigated whether the DNA binding ability of AR was affected by PGC-1α manipulation. The PSA enhancer and promoter regions contained three AREs known as ARE I, ARE II, and ARE III (Fig. 6A). When the samples from LNCaP cells immunoprecipitated with anti-AR antibody were amplified using ARE-containing primer pairs, PCR products were abundant when the primer pairs A/B, C/D, and G/H were used, but not when the primer pairs E/F and I/J were used. Also, the binding of AR to ARE was decreased by the withdrawal of androgen (39) according to withdrawal duration. Similar to a previous report that AR gradually dissociated with DHT and exported to cytoplasm by androgen withdrawal (40), androgen withdrawal for 4 and 16 h reduced AR binding to PSA A/B, C/D, and G/H by approximately 30 and 60%, respectively. Furthermore, when PGC-1α expression was down-regulated by transfecting LNCaP cells with PGC-1α-specific siRNAs, the binding of AR to ARE within the PSA enhancer and promoter regions was reduced (Fig. 6B). These results were confirmed using conventional PCR method (see supplemental Fig. 1A published as supplemental data on The Endocrine Society's Journals Online web site at http://mend.endojournals.org). Similar results were obtained also in CxR cells by both quantitative real-time PCR and conventional PCR methods, although AR binding to ARE in CxR cells was less affected by androgen deprivation (Fig. 6C and supplemental Fig. 1B).

Knock-down of PGC-1α represses cell proliferation in androgen-dependent and CRPC cells

The finding that PGC-1α was involved in a regulation of transcriptional activity of AR prompted us to examine whether PGC-1α might affect the proliferation of PCa cells through modulation of AR function. First, we investigated the proliferation of LNCaP cells transfected with PGC-1α-specific siRNAs in medium containing 1 nM or 10 nM of DHT, or not containing. When PGC-1α was knocked down, cell proliferations in both media were significantly reduced in the presence of DHT, but not in the absence of DHT (Fig. 7A). These results were similar to those with AR knock-down (data not shown). To clarify the mechanism of cell growth retardation by PGC-1α knock-down, we performed flow cytometry analysis for cell-cycle analysis. As shown in Fig. 7B, androgen deprivation induced cell-cycle arrest at G_1 phase. Also, PGC-1α knock-down in medium containing 1 nM or 10 nM of DHT induced cell-cycle arrest at the G_1 phase, but not in medium not containing DHT similar to that with AR knock-down (data not shown); thus, decreasing cell proliferation. However, PGC-1α knock-down in CRPC

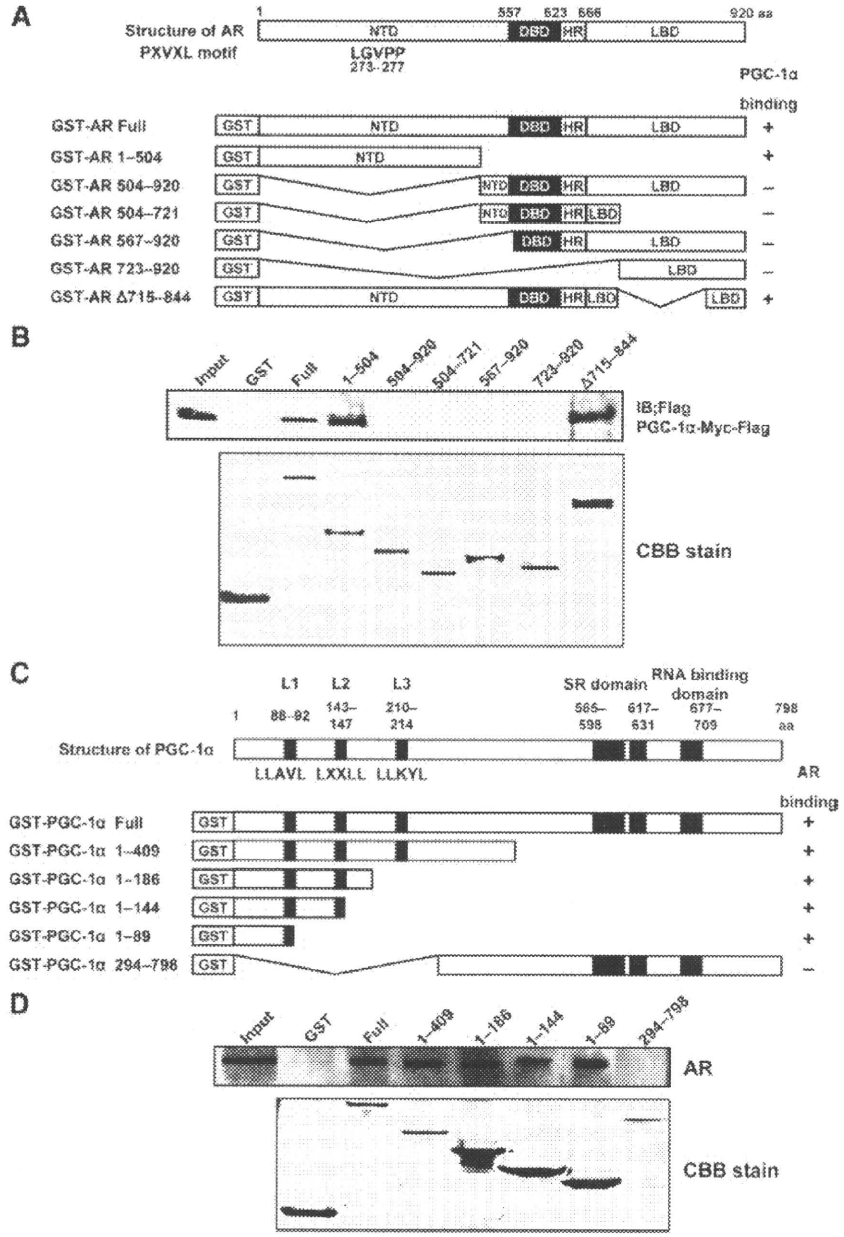

FIG. 4. The NTD of PGC-1α interacts with the TAD of AR. A, Schematic representation of the GST-AR deletion mutants. B, Equal amounts of GST, GST-AR, and various GST-AR deletion mutant fusion proteins, as shown in A, were immobilized on glutathione-sepharose 4B and were incubated with nuclear extracts from PC-3 cells transfected with PGC-1α-Myc-Flag expression plasmid. The bound protein samples and 10% of the input were subjected to SDS-PAGE, and Western blot analysis was performed using an anti-Flag antibody. Purified GST, GST-AR, and GST-AR deletion mutant fusion proteins stained with CBB are also shown. C, Schematic representation of GST-PGC-1α deletion mutants. D, Equal amounts of GST, GST-PGC-1α, and various GST-PGC-1α deletion mutant fusion proteins shown in C, immobilized on glutathione-sepharose 4B, were incubated with nuclear extracts from LNCaP cells. Bound protein samples and 10% of input were subjected to SDS-PAGE, and Western blot analysis was performed using an anti-AR antibody (C-19). Purified GST, GST-PGC-1α, and GST-PGC-1α deletion mutant fusion proteins stained with Coomassie Brilliant Blue (CBB) are also shown. IB, Immunoblots.

cells with no AR expression, PC-3 cells, affected cell proliferation to a lesser extent than that in LNCaP cells. In addition, under androgen starvation, the growth of PC-3 cells was similar to that in medium containing androgens. When PGC-1α was knocked down, PC-3 cell growth in the androgen-deficient medium was similar to that in androgen-containing medium (Fig. 7C). CxR cells are derived from LNCaP cells and exhibit high expression of AR proteins compared with their parental cells, as shown in Fig. 2D. Overexpression of AR has been thought to promote CRPC cell growth, even under androgen starvation by augmentation of AR signaling. Because CxR cells exhibit enhanced AR expression, blockade of AR signaling may be effective to inhibit cell proliferation in CxR cells. As expected, PGC-1α knock-down in CxR delayed cell growth slightly more effectively than that in parental LNCaP cells, most likely by blocking AR signaling both in the absence and presence of DHT (Fig. 7D).

Discussion

Coactivators can interact with and enhance the transcriptional activity of ligand-bound or ligand-unbound AR, and some coactivators are overexpressed in PCa, suggesting that coactivators of AR might be involved in prostate carcinogenesis (41, 42). Various studies have shown that steroid receptors, particularly AR, have pivotal roles in all stages of prostate carcinogenesis (3, 43). Because the activity of steroid receptors is potentiated by a variety of coactivators, it is reasonable to believe that these proteins may also be involved in prostate carcinogenesis (44, 45). Indeed, recent studies have shown that the mRNA of some steroid receptor coactivators is overexpressed in PCa tissues and cell lines (46). The first *bona fide* steroid hormone receptor coactivator, SRC-1, was identified by virtue of its ability to interact with the hormone binding domain of agonist-activated progesterone receptor (47). Subsequently, it was shown that SRC-1 was able to interact efficiently with most nuclear receptors. SRC-3 was first isolated as a steroid receptor coactivator. Recently, it was reported that SRC-3 was overexpressed in PCa spec-

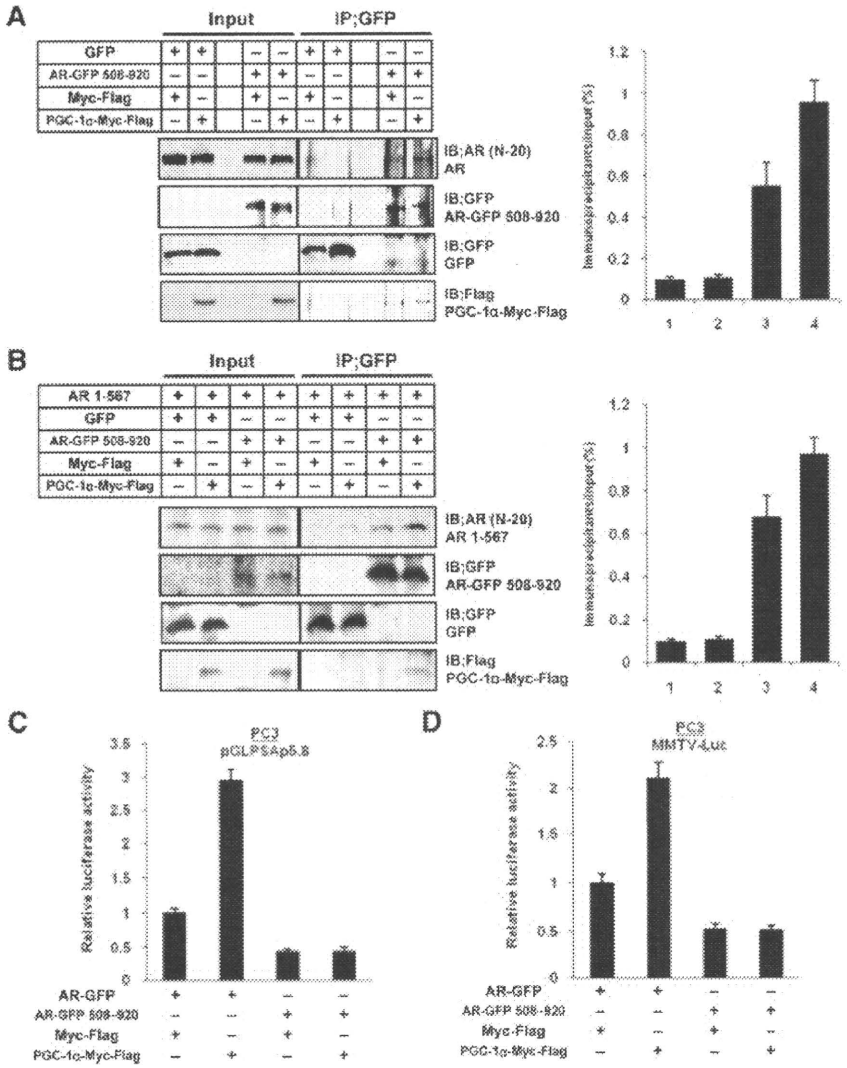

FIG. 5. The TAD of AR is indispensable for the augmentation of AR transcriptional activity by PGC-1α. A, LNCaP cells were cotransfected with 1.0 μg of each of the indicated expression plasmids and were incubated for 48 h. Whole-cell extracts (300 μg) were immunoprecipitated (IP) with agarose-conjugated anti-GFP antibody. The resulting immunocomplexes and whole-cell extracts (30 μg) were subjected to SDS-PAGE, and Western blot analysis was performed using anti-AR (N-20), anti-GFP, and anti-Flag antibodies. The signal intensities for AR protein of coimmunoprecipitated samples were corrected for the results of the corresponding preimmunoprecipitated samples. All values represent at least three independent experiments. Lane 1, GFP and Myc-Flag; lane 2, GFP and PGC-1α-Myc-Flag; lane 3, AR-GFP 508-920 and Myc-Flag; lane 4, AR-GFP 508-920 and PGC-1α-Myc-Flag. *Boxes*, mean; *bars*, ± SD. B, PC-3 cells were cotransfected with 0.65 μg of each of the indicated expression plasmids and were incubated for 48 h. Coimmunoprecipitation assay and Western blot analysis were performed as described in A. The signal intensities for AR 1-567 protein of coimmunoprecipitated samples were corrected for the results of the corresponding preimmunoprecipitated samples. All values represent at least three independent experiments. Lane 1, GFP and Myc-Flag; lane 2, GFP and PGC-1α-Myc-Flag; lane 3, AR-GFP 508-920 and Myc-Flag; lane 4, AR-GFP 508-920 and PGC-1α-Myc-Flag. *Boxes*, Mean; *bars*, ± SD. C and D, PC-3 cells were transiently transfected with 0.33 μg of pGLPSAp5.8 (C) or MMTV-Luc (D), 0.33 μg of Myc-Flag or PGC-1α-Myc-Flag, 0.33 μg of the AR-GFP or AR-GFP 508-920, and 0.05 μg of pRL-TK and incubated in charcoal-stripped medium with 10 nM of DHT for 48 h. *Firefly* luciferase activity was corrected for the corresponding *Renilla* luciferase activity. All values represent at least three independent experiments. The luciferase activity of each reporter plasmid with the AR-GFP and Myc-Flag expression plasmids transfection corresponds to 1. *Boxes*, mean; *bars*, ± SD. IB, Immunoblots.

imens, and its overexpression was correlated with PCa proliferation and is inversely correlated with apoptosis (48). AR coactivators are also involved in castration-resistant progression of PCa, which is critical for advanced PCa patients (49, 50). In this study, PGC-1α was revealed to be overexpressed in PCa cells.

PGC-1α was originally identified as a transcriptional coactivator of PPARγ, and it was determined that PGC-1α also interacts with other nuclear receptors (26, 29). These findings suggest that PGC-1α might also interact with AR and may be involved in carcinogenesis and the progression to CRPC. Therefore, we investigated the interaction between PGC-1α and AR using a GST pull-down assay *in vitro* and coimmunoprecipitation assay *in vivo*. As expected, PGC-1α interacted with AR, and enhanced the transcriptional activity of AR target genes, PSA, and MMTV. Also, we determined the regions of PGC-1α and AR that interact with each other. The results indicate that the NTD of PGC-1α interacts with the TAD of AR. The NTD of PGC-1α contains three LXXLL-like motifs resembling an LXXLL motif, which is known to mediate the recruitment of the p160-type of coactivators to nuclear receptors (51). Mutations of LXXLL motif have been shown to disrupt its interactions with nuclear receptors and abolish its coactivator function (51–53). However, our result showed that deletion mutant of PGC-1α (GST-PGC-1α 1-89) not containing complete LXXLL motif could also interacted with AR. This result indicates that LXXLL motif may be unnecessary for PGC-1α to interact with AR. Otherwise, LL portion (amino acids 88-89) of LXXLL motif may be sufficient to interact with AR.

After determining the region of PGC-1α that interacts with AR, we investigated the region of AR that interacts with PGC-1α. It was shown that PGC-1α interacts with the hinge region or the NTD of nuclear receptors, but

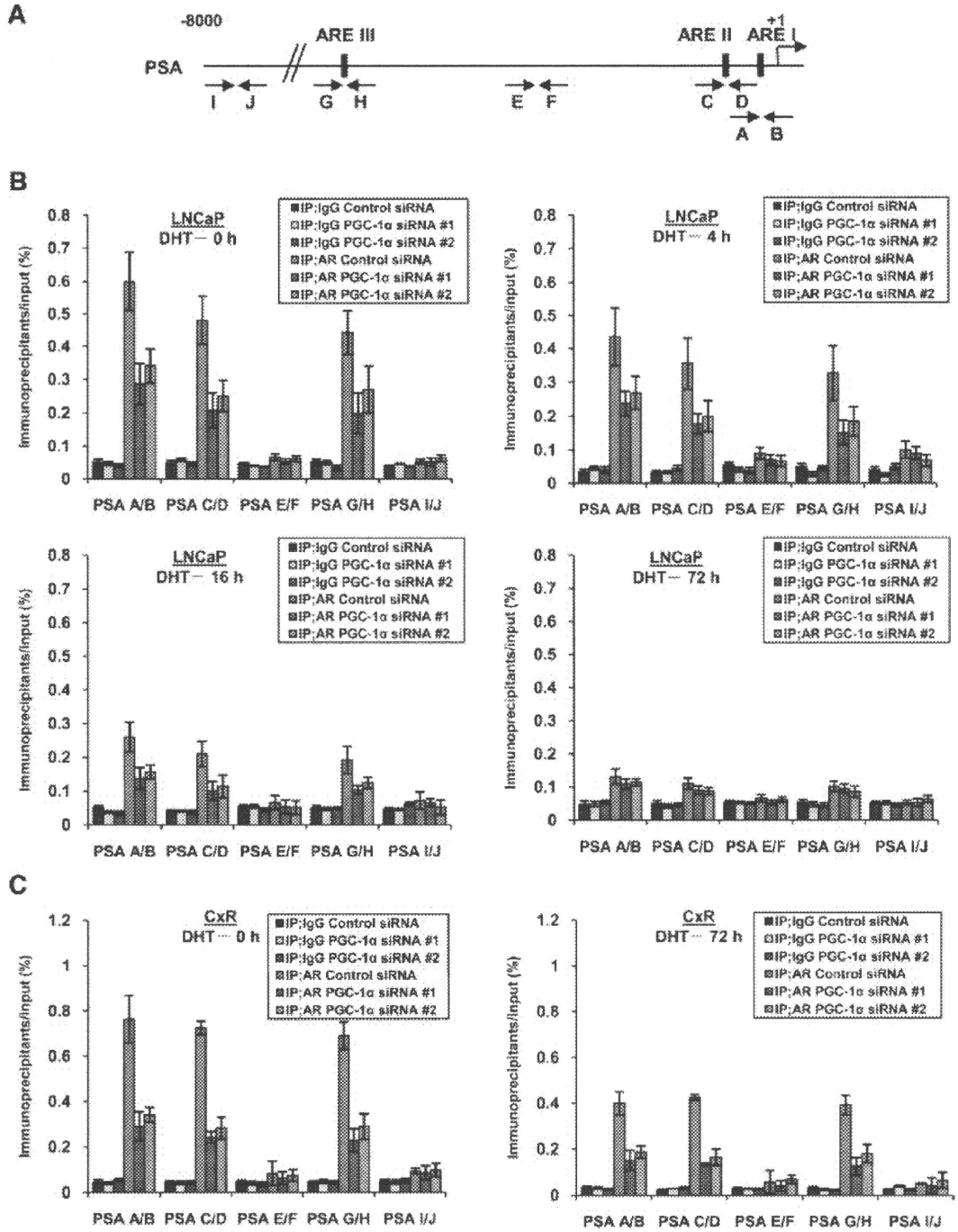

FIG. 6. Knock-down of PGC-1α decreases the DNA-binding ability of AR. A, *Black boxes* and *black arrows* indicate the AREs and PCR primer regions, respectively. B and C, LNCaP (B) and CxR (C) cells were transfected with 50 nM of control siRNA, PGC-1α siRNA no. 1 or PGC-1α siRNA no. 2, and incubated for 72 h. The medium was exchanged from charcoal-stripped medium with 10 nM of DHT into medium without DHT at the indicated time before harvest. The nuclear extracts were then immunoprecipitated (IP) with 2.0 μg of rabbit IgG or anti-AR antibody (C-19) and 20 μl of protein A/G agarose. The quantitative real-time PCR was performed using soluble chromatin, immunoprecipitated DNAs, and the indicted primer pairs. The results of immunoprecipitated samples were corrected for the results of the corresponding soluble chromatin samples. All values represent at least three independent experiments. *Boxes*, Mean; *bars*, ± SD.

the domains of the nuclear receptors that interact with PGC-1α differed between nuclear receptors and between investigators (31, 54, 55). In our experiment, the TAD of AR interacted with PGC-1α. This result is supported by our finding that the interaction between AR and PGC-1α was not affected with or without androgen, suggesting that the LBD of AR was not involved in this interaction. Furthermore, our finding that deletion of the TAD of AR abolished the coactivator function of PGC-1α supported our finding that the TAD of AR is a region that interacts with the PGC-1α. This interaction up-regulated the transactivating ability of AR through the following mecha-

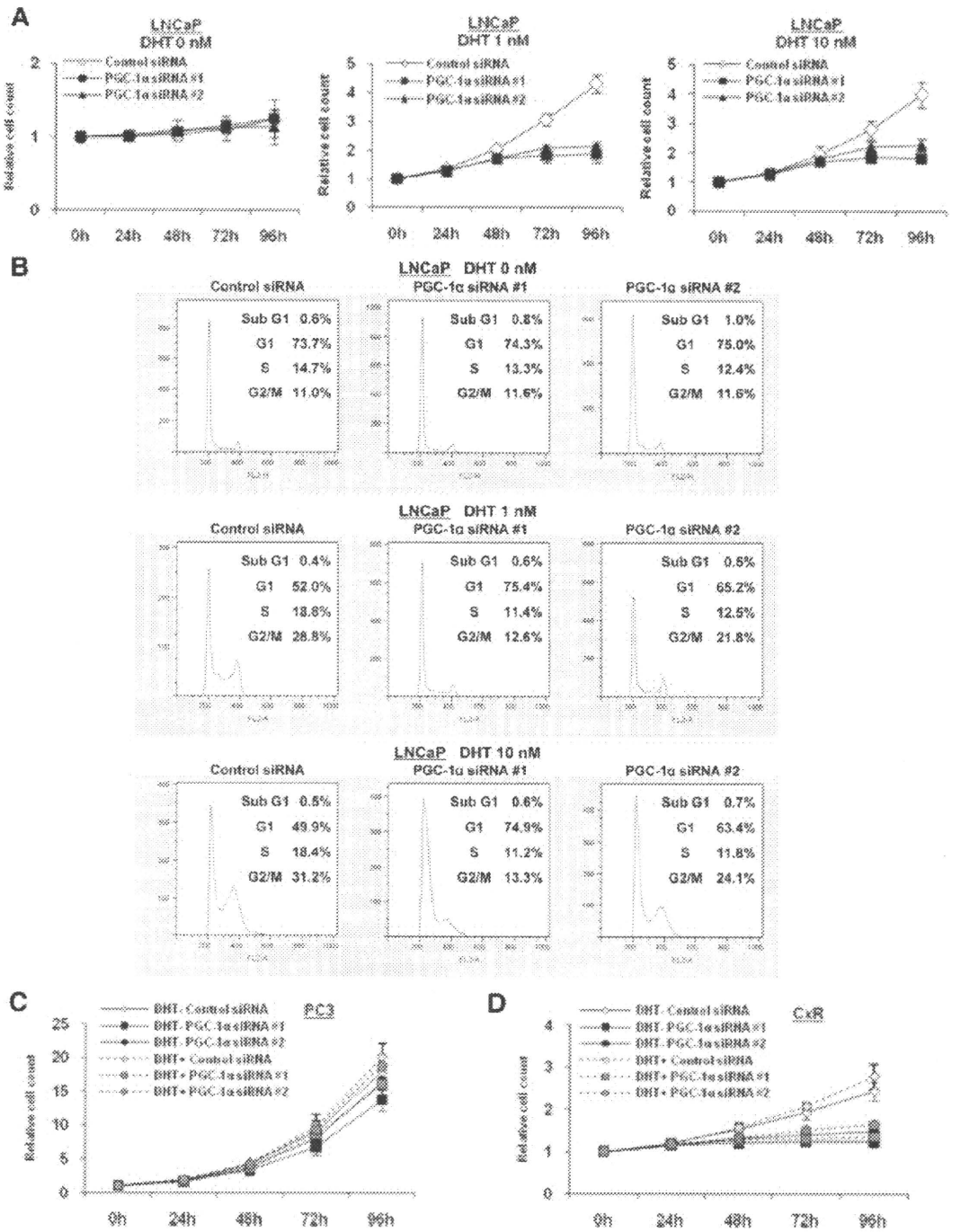

FIG. 7. Knock-down of PGC-1α suppresses cell proliferation in androgen-dependent and CRPC cells. A, LNCaP cells were transiently transfected with 50 nM of control siRNA, PGC-1α siRNA no. 1 or PGC-1α siRNA no. 2, and incubated in charcoal-stripped medium with 0, 1, or 10 nM of DHT. The cell numbers were counted at the indicated times. The results were normalized to cell numbers at hour 0. All values represent at least three independent experiments. *Boxes*, mean; *bars*, ± SD. B, LNCaP cells were transiently transfected with 50 nM of control siRNA, PGC-1α siRNA no. 1 or PGC-1α siRNA no. 2, and incubated in charcoal-stripped medium with 0, 1, or 10 nM of DHT. Seventy-two hours after transfection, the cells were stained with propidium iodide and analyzed by flow cytometry. The cell cycle fraction is shown in the *right upper* position of each graph. C and D, PC-3 (C) and CxR (D) cells were transiently transfected with 50 nM of control siRNA, PGC-1α siRNA no. 1 or PGC-1α siRNA no. 2, and incubated in charcoal-stripped medium with or without 10 nM of DHT. The cell proliferation assay was performed as described in A. *Boxes*, Mean; *bars*, ± SD.

nism. As indicated in Figs. 5 and 6, the interaction between PGC-1α and AR augmented the formation of a AR homodimer, leading to enhanced AR binding to the ARE and the expression of AR target genes.

Wirtenberger *et al.* (35) previously reported that the PGC-1α Thr612Met polymorphism was associated with familial breast cancer, high-risk familial breast cancer, and bilateral familial breast cancer risk in patients not carrying the BRCA 1/2 mutation (35). This finding suggests that PGC-1α function is involved in breast cancer carcinogenesis and progression by acting as a coactivator of ER. Therefore, we hypothesized that PGC-1α might

also be involved in carcinogenesis and the progression of PCa, and investigated the effect of PGC-1α expression manipulation on androgen-dependent and CRPC cell growth. Our results showed that PGC-1α knock-down suppressed the growth of PCa cells. In particular, PGC-1α knock-down suppressed growth and cell-cycle arrest at the G_1 phase in AR-expressing PCa cells more effectively compared with PCa cells with no AR expression. This finding suggests that PGC-1α predominantly acts on PCa cells, at least in part, by interacting with and acting as a coactivator for AR. Although PC-3 cells expressing no AR mRNA and protein were also little affected by PGC-1α knock-down in the presence and absence of androgen, these effects may result from other functions of PGC-1α as other nuclear receptor coactivators, which was confirmed by the finding that cell growth suppression by PGC-1α knock-down was not affected by androgen depletion.

Also, PGC-1α and AR signaling are known to modulate metabolic activity. AR-null mice exhibit metabolic disease-like phenotype (56, 57). Similarly, PGC-1α knock-down reduced lipid metabolism, leading to storage of fat in adipocyte (58). Moreover, SRC-3, an AR coactivator was recently shown to induce PGC-1α acetylation and consequently inhibit its activity. Ablation of SRC-3 was subsequently found to improve insulin sensitivity (59). These findings support our results that PGC-1α interacts with AR and influences AR signaling. In addition, PGC-1α and AR signaling might be a useful therapeutic target for metabolic disease.

In conclusion, PGC-1α interacted with AR and activated the transcriptional function of AR. Also, PGC-1α knock-down delayed cell growth in AR expressing PCa cells. Furthermore, in castration-resistant LNCaP derivatives, CxR cells, PGC-1α knock-down suppressed cellular proliferation. Although PGC-1α expression needs to be investigated in PCa tissues compared with normal prostate glands, these findings indicate that the modulation of PGC-1α expression or function might be a useful strategy for developing novel therapeutics in PCa, which usually depends on androgens. Also, this strategy might be more useful for CRPC cells, which depends on AR signaling.

Materials and Methods

Cell culture

Human normal prostate epithelium RWPE-1 (keratinocyte serum-free medium), Human PCa DU145 (DMEM), PC-3 (Eagle's MEM), VCaP (DMEM), 22Rv1 (RPMI1640), and LNCaP cells (RPMI1640) were cultured in the indicated media. These media were purchased from Invitrogen (San Diego, CA) and contained 10% fetal bovine serum. LNCaP cells propagated between 10 and 30 times were used. Castration-resistant derivatives of LNCaP cells, LNCaP-CxR cells (referred to as CxR cells), were established and maintained as previously described (60). The cell lines were maintained in a 5% CO_2 atmosphere at 37°C.

Antibodies

Antibodies against AR (C-19, sc-815), AR (N-20, sc-7305), PSA (sc-7316), GFP (sc-8334), PGC-1α (sc-13067), and agarose-conjugated anti-GFP antibody (sc-8334 AC) were purchased from Santa Cruz Biotechnology (Santa Cruz, CA). Anti-Flag (M2) and anti-β-actin antibodies were purchased from Sigma (St. Louis, MO).

Plasmid construction

The AR-GFP plasmid expressing C-terminally GFP-tagged AR protein was kindly provided by T. Yanase (Fukuoka University, Fukuoka, Japan) (61). The pCMV-AR plasmid expressing wild-type AR, pCMV-ARmut877 plasmid expressing mutated AR (T877A), and MMTV-Luc were kindly provided by C. Chang (University of Rochester, Rochester, NY). The pGLP-SAp5.8 was kindly provided by A. Mizokami (Kanazawa University, Kanazawa, Japan) (62). To construct the AR-GFP 508-920 plasmid expressing GFP-tagged N-terminal deleted AR protein (from 508 to 920 aa), PCR was carried out with AR-GFP as a template using the following primer pairs: 5′-GCTAGCGGTACCCTGGCGGCATGGTGA-3′ and 5′-GGATCCACTGGGTGTGGAAATAGATGG-3′. The PCR product was cloned into the pEGFP vector (Clontech, Mountain View, CA). pCMV-AR 1-567 expressing C-terminal deleted AR protein (1-567 aa) was constructed by deletion of *Hin*dIII fragment from pCMV-AR plasmid. To obtain the full-length cDNA for AR, PCR was carried out with pCMV-AR as a template using the following primer pairs: 5′-ATGGAAGTG-CAGTTAGGGCTGG-3′ and 5′-TCACTGGGTGTG-GAAATAGATG-3′. The PCR product was cloned into the pGEM-T easy vector (Promega, Madison, WI). To construct pGEX-AR expressing GST-AR, a fragment of AR cDNA was ligated into the pGEX plasmid (GE Healthcare Bio-Science, Piscataway, NJ). The GST-AR deletion mutants (GST-AR 1-504, GST-AR 504-920, GST-AR 567-920, GST-AR 723-920, and GST-AR Δ715-844) were constructed from pGEX-AR full-length plasmid by deletion of the *Sph*I-*Acc*65I, *Acc*65I-*Hin*dIII, *Bam*HI-*Hin*dIII, *Sal*I-*Eco*RI, and *Bsr*GI fragments, respectively. GST-AR 504-721 was created from GST-AR 504-920 by deletion of the *Stu*I-*Not*I fragment.

The PGC-1α-Myc-Flag plasmid expressing the C-terminally Myc-Flag-tagged PGC-1α protein was purchased from OriGene (Rockville, MD). To obtain the full-length cDNA for PGC-1α, PCR was carried out with the PGC-1α-Myc-Flag plasmid as a template using the following primer pairs: 5′-GATGGCGTGG-GACATGTGCAACCA-3′ and 5′-TTACCTGCGCAAGCT-TCTCTGAGC-3′. The PCR product was cloned into the pGEM-T easy vector. To construct pGEX-PGC-1α expressing GST-PGC-1α, a fragment of PGC-1α cDNA was ligated into the pGEX plasmid. GST-PGC-1α deletion mutants (GST-PGC-1α 1-409, GST-PGC-1α 1-144, GST-PGC-1α 1-89, and GST-PGC-1α 294-798) were constructed from pGEX-PGC-1α full-length plasmid by deletion of the *Xba*I-*Not*I, *Afl*II-*Not*I, *Nhe*I-*Not*I, and *Bam*HI-*Stu*I fragments, respectively. To construct GST-PGC-1α 1-186, N-terminal *Eco*RI fragment of cDNA for PGC-1α was ligated into the pGEX plasmid.

Western blot analysis

Whole-cell lysates and nuclear extracts were prepared as previously described (60, 63–66). The protein concentration of the extracts was quantified using a Protein Assay kit based on the Bradford method (Bio-Rad, Hercules, CA). The indicated amounts of whole-cell lysates and nuclear extracts were separated by 4–20% SDS-PAGE and transferred to polyvinylidene difluoride microporous membranes (GE Healthcare Bio-Science) using a semidry blotter. The blotted membranes were incubated for 1 h at room temperature with the primary antibodies described above. The membranes were then incubated for 40 min at room temperature with a peroxidase-conjugated secondary antibody. The bound antibody was visualized using an ECL kit (GE Healthcare Bio-Science), and the membranes were exposed to Kodak X-OMAT film.

Expression of GST-fusion proteins in *Escherichia coli*

GST-fusion proteins in *E. coli* were prepared as previously described (64–66). To express GST-fusion proteins, bacteria transformed with expression plasmids were incubated with 1 mM isopropyl-β-D-thiogalactopyranoside (Nacalai tesque, Kyoto, Japan) for 2 h at room temperature and collected by centrifugation. The cells were sonicated (TAITEC sonicator, Tokyo, Japan) in buffer X containing 50 mM Tris-HCl (pH 8.0), 1 mM EDTA, 120 mM NaCl, 0.5% (vol/vol) Nonidet P-40 (NP-40), 10% (vol/vol) glycerol, 1 mM phenylmethylsulfonyl fluoride, and 1 mM dithiothreitol, and the cell lysates were collected after centrifugation at 21,000 *g* for 10 min at 4°C.

GST pull-down assay

The GST pull-down assay was performed as previously described (64–66). GST-AR, GST-PGC-1α, or their deletion mutants immobilized on glutathione-sepharose 4B (GE Healthcare Bio-Science) were incubated with soluble cell extracts for 2 h at 4 C in buffer X. The bound samples were washed three times with buffer X and subjected to Western blot analysis with the indicated antibodies.

Coimmunoprecipitation assay

The transient transfection and immunoprecipitation assays were performed as previously described (64–66). Briefly, 1×10^5 LNCaP and PC-3 cells were transfected with the indicated amounts of each of the indicated expression plasmids using Lipofectamine 2000 (Invitrogen) according to the manufacturer's instructions and seeded into six-well plates. After incubation at 37°C for 48 h with the indicated fresh medium, the cells were lysed in buffer X. The lysates were centrifuged at 21,000 × *g* for 10 min at 4°C, and the supernatants (300 μg) were incubated for 2 h at 4°C with agarose-conjugated anti-GFP antibody. The immunoprecipitated samples were washed three times with buffer X, and the preimmunoprecipitated samples (30 μg) were subjected to Western blot analysis with the indicated antibodies. Signal intensities of preimmunoprecipitated and coimmunoprecipitated AR protein were quantified using the NIH Imaging program (NIH, Bethesda, MD). The intensities of coimmunoprecipitated AR protein were corrected for the corresponding intensities of preimmunoprecipitated AR protein. The results are representative of at least three independent experiments.

For immunoprecipitation assays without transient transfection, 70–80% confluent LNCaP cells were cultured in 100-mm tissue-culture plates with the indicated medium for 48 h and lysed with buffer X. The lysates were centrifuged at 21,000 × *g* for 10 min at 4 C, and the supernatants (500 μg) were incubated overnight at 4 C with 2.0 μg of rabbit IgG or anti-AR antibody. The immunoprecipitated samples were washed three times with buffer X, and the preimmunoprecipitated samples (50 μg) were subjected to Western blot analysis with the indicated antibodies.

Knock-down analysis using siRNAs

Knock-down analysis using siRNA was performed as previously described (60, 63–66). The following double-stranded RNA 25-base-pair oligonucleotides were commercially generated (Invitrogen): 5′-AAUCUGUGGAAGAACAAAUCUGCCC-3′ (sense) and 5′-GGGCAGAUUUGUUCUUCCACAGAUU-3′ (antisense) for PGC-1α siRNA no. 1; 5′-UAUUCUUCCCUCUUCAGCCUCUCGU-3′ (sense) and 5′-ACGAGAGGCUGAAGAGGGAAGAAUA-3′ (antisense) for PGC-1α siRNA no. 2. LNCaP, CxR and PC-3 cells were transfected with siRNA using Lipofectamine 2000 according to the manufacturer's instructions.

RNA isolation and RT-PCR

Total RNA was prepared from cultured cells using RNeasy mini kits (QIAGEN, Valencia, CA). First-strand cDNA was synthesized from 1.0 μg of total RNA using a Transcriptor First-Strand cDNA Synthesis Kit (Roche Applied Science, Indianapolis, IN) according to the manufacturer's instructions.

Quantitative real-time PCR

The synthesized cDNA was diluted 1:2, and 2.0 μl of the diluted mixture was used. Quantitative real-time PCR with TaqMan Gene Expression Assay (Applied Biosystems, Foster City, CA) and TaqMan Gene Expression Master Mix (Applied Biosystems) was performed using ABI 7900HT (Applied Biosystems). The expression level of AR and PSA mRNA was corrected for the corresponding glyceraldehyde 3-phosphate dehydrogenase (GAPDH) mRNA expression level. The results are representative of at least three independent experiments.

Luciferase reporter assay

The luciferase reporter assay was performed as previously described (60). Briefly, LNCaP and PC-3 cells (1.5×10^5) were cotransfected with the indicated amounts of reporter plasmids, 0.05 μg of pRL-TK as an internal control and the indicated amounts of expression plasmids or siRNA using Lipofectamine 2000 according to the manufacturer's instructions and seeded into 12-well plates. After incubation for 48 h, luciferase activity was detected using a Dual-Luciferase Reporter Assay System (Promega). Light intensity was measured using a plate reader (ARVO™ MX; Perkin Elmer Inc., Waltham, MA). *Firefly* luciferase activity was corrected for the corresponding *Renilla* luciferase activity. The results are representative of at least three independent experiments.

Chromatin immunoprecipitation assay

Chromatin immunoprecipitation assay was performed as previously described (60, 63, 65). Briefly, LNCaP and CxR cells were transfected with control siRNA, PGC-1α siRNA no. 1 or PGC-1α siRNA no. 2, seeded into six-well plates, and incubated for 72 h. Soluble chromatin from 1×10^6 cells was incubated overnight at 4°C with 2.0 μg of antirabbit IgG or anti-AR an-

tibody and 20 μl of protein A/G agarose. Purified DNA was dissolved in 20 μl of dH_2O, and 1 μl of the diluted mixture was used for PCR analysis with the following primer pairs: 5′-TCTGCCTTTGTCCCCTAGAT-3′ (forward) and 5′-AACCTTCATTCCCCAGGACT-3′ (reverse) for PSA A/B (−250 bp to −39 bp); 5′-AGGGATCAGGGAGTCTCACA-3′ (forward) and 5′-GCTAGCACTTGCTGTTCTGC-3′ (reverse) for PSA C/D (−406 bp to −164 bp); 5′-CTGTGCTTGGAGTTTACCTGA-3′ (forward) and 5′-GCAGAGGTTGCAGTGAGCC-3′ (reverse) for PSA E/F (−1997 bp to −1846 bp); 5′-CCTCCCAGGTTCAAGTGATT-3′ (forward) and 5′-GCCTGTAATCCCAGCACTTT-3′ (reverse) for PSA G/H (−4170 bp to −3978 bp); 5′-GATGGTGTTTCACCGTGTTG-3′ (forward) and 5′-AGAGTGCAGTGAGCCGAGAT-3′ (reverse) for PSA I/J (−7694 bp to −7484 bp). These primer pairs were described previously (39). The PCR products were separated by electrophoresis on 2% agarose gels and stained with ethidium bromide. The quantitative real-time PCR assay with 1 μl of the diluted DNA, the above primer pairs and SYBR Premix Ex Taq II (Takara Bio, Shiga, Japan) was performed using ABI 7900HT. The results are representative of at least three independent experiments.

Cell proliferation assay

The cell proliferation assay was performed as previously described (60, 63, 64, 66). Briefly, 2.0×10^4 LNCaP, CxR and PC-3 cells were transfected with control siRNA, PGC-1α siRNA no. 1 or PGC-1α siRNA no. 2, as described above and seeded in 12-well plates, and incubated in the indicated medium. Twelve hours after transfection was set as hour 0. The cells were harvested with trypsin and counted daily using a cell counter (Beckman Coulter, Fullerton, CA). The results were normalized to cell counts at h 0, and are representative of at least three independent experiments.

Flow cytometry analysis

The flow cytometry analysis was performed as previously described (60, 63). Briefly, 2.5×10^5 LNCaP cells were transfected with control siRNA, PGC-1α siRNA no. 1 or PGC-1α siRNA no. 2, seeded in six-well plates, and incubated in the indicated medium for 72 h. The cells were harvested, washed twice with ice-cold PBS with 0.1% BSA, and resuspended in 70% ethanol. After washing twice with ice-cold PBS, the cells were resuspended in PBS with 0.1% BSA, incubated with RNase (Roche Molecular Biochemicals, Basel, Switzerland), and stained with propidium iodide (Sigma). Cells were analyzed using a FACS Calibur (BD Biosciences, San Jose, CA).

Acknowledgments

We thank Dr. Toshihiko Yanase, Dr. Chawnshang Chang, and Dr. Atsushi Mizokami for providing the plasmids; Dr. Dongchon Kang (Kyushu University, Fukuoka, Japan) for helping with quantitative real-time PCR and flow cytometry; and Noriko Hakoda, Hitomi Matoba, and Seiko Kamori for their technical assistance.

Address all correspondence and requests for reprints to: Akira Yokomizo M.D., Ph.D., Department of Urology, Graduate School of Medical Sciences, Kyushu University, 3-1-1 Maidashi, Higashi-ku, Fukuoka 812-8252, Japan. E-mail: yokoa@uro.med.kyushu-u.ac.jp.

This work was supported by Health Sciences Research Grants for Clinical Research for Evidenced Based Medicine and Grant-in-Aid for Cancer Research 016 from the Ministry of Health, Labor, and Welfare, Japan; and by a Young Researcher Promotion grant from the Japanese Urological Association, Japan.

Disclosure Summary: The authors have nothing to disclose.

References

1. **Grönberg H** 2003 Prostate cancer epidemiology. Lancet 361:859–864
2. **Hsing AW, Devesa SS** 2001 Trends and patterns of prostate cancer: what do they suggest? Epidemiol Rev 23:3–13
3. **Feldman BJ, Feldman D** 2001 The development of androgen-independent prostate cancer. Nat Rev Cancer 1:34–45
4. **Han M, Partin AW, Piantadosi S, Epstein JI, Walsh PC** 2001 Era specific biochemical recurrence-free survival following radical prostatectomy for clinically localized prostate cancer. J Urol 186:416–419
5. **Isaacs W, De Marzo A, Nelson WG** 2002 Focus on prostate cancer. Cancer Cell 2:113–116
6. **Debes JD, Tindall DJ** 2002 The role of androgens and the androgen receptor in prostate cancer. Cancer Lett 187:1–7
7. **Scher HI, Sawyers CL** 2005 Biology of progressive, castration-resistant prostate cancer: directed therapies targeting the androgen-receptor signaling axis. J Clin Oncol 23:8253–8261
8. **Gregory CW, Hamil KG, Kim D, Hall SH, Pretlow TG, Mohler JL, French FS** 1998 Androgen receptor expression in androgen-independent prostate cancer is associated with increased expression of androgen-regulated genes. Cancer Res 58:5718–5724
9. **Chen CD, Welsbie DS, Tran C, Baek SH, Chen R, Vessella R, Rosenfeld MG, Sawyers CL** 2004 Molecular determinants of resistance to antiandrogen therapy. Nat Med 10:33–39
10. **Zegarra-Moro OL, Schmidt LJ, Huang H, Tindall DJ** 2002 Disruption of androgen function inhibits proliferation of androgen-refractory prostate cancer cells. Cancer Res 62:1008–1013
11. **Linja MJ, Savinainen KJ, Saramäki OR, Tammela TL, Vessella RL, Visakorpi T** 2001 Amplification and overexpression of androgen receptor gene in hormone-refractory prostate cancer. Cancer Res 61:3550–3555
12. **Taplin ME, Rajeshkumar B, Halabi S, Werner CP, Woda BA, Picus J, Stadler W, Hayes DF, Kantoff PW, Vogelzang NJ, Small EJ** 2003 Androgen receptor mutations in androgen-independent prostate cancer: Cancer and Leukemia Group B Study 9663. J Clin Oncol 21:2673–2678
13. **Culig Z, Hobisch A, Cronauer MV, Radmayr C, Trapman J, Hittmair A, Bartsch G, Klocker H** 1994 Androgen receptor activation in prostate tumor cell lines by insulin-like growth factor-I, keratinocyte growth factor, and epidermal growth factor. Cancer Res 54:5474–5478
14. **Craft N, Shostak Y, Carey M, Sawyers CL** 1999 A mechanism for hormone-independent prostate cancer through modulation of androgen receptor signaling by the HER-2/*neu* tyrosine kinase. Nat Med 5:280–285
15. **Hobisch A, Eder IE, Putz T, Horninger W, Bartsch G, Klocker H, Culig Z** 1998 Interleukin-6 regulates prostate-specific protein expression in prostate carcinoma cells by activation of the androgen receptor. Cancer Res 58:4640–4645
16. **Zoubeidi A, Zardan A, Beraldi E, Fazli L, Sowery R, Rennie P, Nelson C, Gleave M** 2007 Cooperative interaction between androgen receptor (AR) and heat-shock protein 27 facilitate AR transcriptional activity. Cancer Res 67:10455–10465
17. **Park SY, Yu X, Ip C, Mohler JL, Bogner PN, Park YM** 2007 Peroxiredoxin 1 interacts with androgen receptor and enhances its transactivation. Cancer Res 67:9294–9303

18. Gaughan L, Logan IR, Cook S, Neal DE, Robson CN 2002 Tip60 and histone deacetylase 1 regulate androgen receptor activity through changes to the acetylation status of the receptor. J Biol Chem 277:25904–25913
19. Miyamoto H, Rahman M, Takatera H, Kang HY, Yeh S, Chang HC, Nishimura K, Fujimoto N, Chang C 2002 A dominant-negative mutant of androgen receptor coregulator ARA-54 inhibits androgen receptor-mediated prostate cancer growth. J Biol Chem 277:4609–4617
20. Fujimoto N, Yeh S, Kang HY, Inui S, Chang HC, Mizokami A, Chang C 1999 Cloning and characterization of androgen receptor coactivator, ARA55, in human prostate. J Biol Chem 274:8316–8321
21. Rahman MM, Miyamoto H, Taketera H, Yeh S, Altuwaijri S, Chang C 2003 Reducing the agonist activity of antiandrogens by a dominant-negative androgen receptor coregulator ARA70 in prostate cancer cells. J Biol Chem 278:19619–19626
22. Hong H, Kohli K, Garabedian MJ, Stallcup MR 1997 GRIP1, a transcriptional coactivator for the AF-2 transactivation domain of steroid, thyroid, retinoid, and vitamin D receptors. Mol Cell Biol 17:2735–2744
23. Boonyaratanakornkit V, Melvin V, Prendergast P, Altmann M, Ronfani L, Bianchi ME, Taraseviciene L, Nordeen SK, Allegretto EA, Edwards DP 1998 High-mobility group chromatin proteins 1 and 2 functionally interact with steroid hormone receptors to enhance their DNA binding in vitro and transcriptional activity in mammalian cells. Mol Cell Biol 18:4471–4487
24. Gross M, Liu B, Tan J, French FS, Carey M, Shuai K 2001 Distinct effects of PIAS proteins on androgen-mediated gene activation in prostate cancer cells. Oncogene 20:3880–3887
25. Bevan CL, Hoare S, Claessens F, Heery DM, Parker MG 1999 The AF1 and AF2 domains of the androgen receptor interact with distinct regions of SRC1. Mol Cell Biol 19:8383–8392
26. Puigserver P, Wu Z, Park CW, Graves R, Wright M, Spiegelman BM 1998 A cold-inducible coactivator of nuclear receptors linked to adaptive thermogenesis. Cell 92:829–839
27. Knutti D, Kaul A, Kralli A 2000 A tissue-specific coactivator of steroid receptors, identified in a functional genetic screen. Mol Cell Biol 20:2411–2422
28. Wu Z, Puigserver P, Andersson U, Zhang C, Adelmant G, Mootha V, Troy A, Cinti S, Lowell B, Scarpulla RC, Spiegelman BM 1999 Mechanisms controlling mitochondrial biogenesis and respiration through the thermogenic coactivator PGC-1. Cell 98:115–124
29. Kressler D, Schreiber SN, Knutti D, Kralli A 2002 The PGC-1-related protein PERC is a selective coactivator of estrogen receptor α. J Biol Chem 277:13918–13925
30. Tcherepanova I, Puigserver P, Norris JD, Spiegelman BM, McDonnell DP 2000 Modulation of estrogen receptor-α transcriptional activity by the coactivator PGC-1. J Biol Chem 275:16302–16308
31. Bourdoncle A, Labesse G, Margueron R, Castet A, Cavaillès V, Royer CA 2005 The nuclear receptor coactivator PGC-1α exhibits modes of interaction with the estrogen receptor distinct from those of SRC-1. J Mol Biol 347:921–934
32. Castillo G, Brun RP, Rosenfield JK, Hauser S, Park CW, Troy AE, Wright ME, Spiegelman BM 1999 An adipogenic cofactor bound by the differentiation domain of PPARγ. EMBO J 18:3676–3687
33. Anderson E 2002 The role of oestrogen and progesterone receptors in human mammary development and tumorigenesis. Breast Cancer Res 4:197–201
34. Fishman J, Osborne MP, Telang NT 1995 The role of estrogen in mammary carcinogenesis. Ann NY Acad Sci 768:91–100
35. Wirtenberger M, Tchatchou S, Hemminki K, Schmutzhard J, Sutter C, Schmutzler RK, Meindl A, Wappenschmidt B, Kiechle M, Arnold N, Weber BH, Niederacher D, Bartram CR, Burwinkel B 2006 Association of genetic variants in the estrogen receptor coactivators PPARGC1A, PPARGC1B and EP300 with familial breast cancer. Carcinogenesis 27:2201–2208
36. Shenk JL, Fisher CJ, Chen SY, Zhou XF, Tillman K, Shemshedini L 2001 p53 Represses androgen-induced transactivation of prostate-specific antigen by disrupting hAR amino- to carboxyl-terminal interaction. J Biol Chem 42:38472–38479
37. Li J, Fu J, Toumazou C, Yoon HG, Wong J 2006 A role of the amino-terminal (N) and carboxyl-terminal (C) interaction in binding of androgen receptor to chromatin. Mol Endocrinol 20:776–785
38. Need EF, Scher HI, Peters AA, Moore NL, Cheong A, Ryan CJ, Wittert GA, Marshall VR, Tilley WD, Buchanan G 2009 A novel androgen receptor amino terminal region reveals two classes of amino/carboxyl interaction-deficient variants with divergent capacity to activate responsive sites in chromatin. Endocrinology 150:2674–2682
39. Shang Y, Myers M, Brown M 2002 Formation of the androgen receptor transcription complex. Mol Cell 9:601–610
40. Tyagi RK, Lavrovsky Y, Ahn SC, Song CS, Chatterjee B, Roy AK 2000 Dynamics of intracellular movement and nucleocytoplasmic recycling of the ligand-activated androgen receptor in living cells. Mol Endocrinol 14:1162–1174
41. Debes JD, Sebo TJ, Lohse CM, Murphy LM, Haugen DA, Tindall DJ 2003 p300 In prostate cancer proliferation and progression. Cancer Res 63:7638–7640
42. Powell SM, Christiaens V, Voulgaraki D, Waxman J, Claessens F, Bevan CL 2004 Mechanisms of androgen receptor signaling via steroid receptor coactivator-1 in prostate. Endocr Relat Cancer 11:117–130
43. Abate-Shen C, Shen MM 2000 Molecular genetics of prostate cancer. Genes Dev 14:2410–2434
44. McKenna NJ, Lanz RB, O'Malley BW 1999 Nuclear receptor coregulators: cellular and molecular biology. Endocr Rev 29:321–344
45. McKenna NJ, O'Malley BW 2002 Combined control of gene expression by nuclear receptors and coregulators. Cell 108:465–474
46. Linja MJ, Porkka KP, Kang Z, Savinainen KJ, Jänne OA, Tammela TL, Vessella RL, Palvimo JJ, Visakorpi T 2004 Expression of androgen receptor coregulators in prostate cancer. Clin Cancer Res 10:1032–1040
47. Oñate SA, Tsai SY, Tsai MJ, O'Malley BW 1995 Sequence and characterization of a coactivator for the steroid hormone receptor superfamily. Science 270:1354–1357
48. Zhou HJ, Yan J, Luo W, Ayala G, Lin SH, Erdem H, Ittmann M, Tsai SY, Tsai MJ 2005 SRC-3 is required for prostate cancer cell proliferation and survival. Cancer Res 65:7976–7983
49. Shi XB, Xue L, Zou JX, Gandour-Edwards R, Chen H, deVere White RW 2008 Prolonged androgen receptor loading onto chromatin and the efficient recruitment of p160 coactivators contribute to androgen-independent growth of prostate cancer cells. Prostate 68:1816–1826
50. Heemers HV, Sebo TJ, Debes JD, Regan KM, Raclaw KA, Murphy LM, Hobisch A, Culig Z, Tindall DJ 2007 Androgen deprivation increases p300 expression in prostate cancer cells. Cancer Res 67:3422–3430
51. Heery DM, Kalkhoven E, Hoare S, Parker MG 1997 A signature motif in transcriptional co-activators mediates binding to nuclear receptors. Nature 387:733–736
52. Voegel JJ, Heine MJ, Tini M, Vivat V, Chambon P, Gronemeyer H 1998 The coactivator TIF2 contains three nuclear receptor-binding motifs and mediates transactivation through CBP binding-dependent and -independent pathways. EMBO J 17:507–519
53. McInerney EM, Weis KE, Sun J, Mosselman S, Katzenellenbogen BS 1998 Transcription activation by the human estrogen receptor subtype β (ERβ) studied with ERβ and ERα receptor chimeras. Endocrinology 139:4513–4522
54. Greschik H, Althage M, Flaig R, Sato Y, Chavant V, Peluso-Iltis C, Choulier L, Cronet P, Rochel N, Schüle R, Strömstedt PE, Moras D 2008 Communication between the ERRα homodimer interface and the PGC-1α binding surface via the helix 8–9 loop. J Biol Chem 283:20220–20230
55. Delerive P, Wu Y, Burris TP, Chin WW, Suen CS 2002 PGC-1

functions as a transcriptional coactivator for the retinoid X receptors. J Biol Chem 277:3913–3917
56. **Sato T, Otaka M, Odashima M, Kato S, Jin M, Konishi N, Matsuhashi T, Watanabe S** 2006 Specific type IV phosphodiesterase inhibitor ameliorates cerulein-induced pancreatitis in rats. Biochem Biophys Res Commun 346:339–344
57. **Yanase T, Fan W, Kyoya K, Min L, Takayanagi R, Kato S, Nawata H** 2008 Androgens and metabolic syndrome: lessons from androgen receptor knock out (ARKO) mice. J Steroid Biochem Mol Biol 109:254–257
58. **Sanyal S, Matthews J, Bouton D, Kim HJ, Choi HS, Treuter E, Gustafsson JA** 2004 Deoxyribonucleic acid response element-dependent regulation of transcription by orphan nuclear receptor estrogen receptor-related receptor γ. Mol Endocrinol 18:312–325
59. **Coste A, Louet JF, Lagouge M, Lerin C, Antal MC, Meziane H, Schoonjans K, Puigserver P, O'Malley BW, Auwerx J** 2008 The genetic ablation of SRC-3 protects against obesity and improves insulin sensitivity by reducing the acetylation of PGC-1α. Proc Natl Acad Sci USA 105:17187–17192
60. **Shiota M, Yokomizo A, Tada Y, Inokuchi J, Kashiwagi E, Masubuchi D, Eto M, Uchiumi T, Naito S,** Castration resistance of prostate cancer cells caused by castration-induced oxidative stress through Twist1 and androgen receptor overexpression. Oncogene 10.1038/onc.2009.322
61. **Tomura A, Goto K, Morinaga H, Nomura M, Okabe T, Yanase T, Takayanagi R, Nawata H** 2001 The subnuclear three-dimensional image analysis of androgen receptor fused to green fluorescence protein. J Biol Chem 276:28395–28401
62. **Mizokami A, Gotoh A, Yamada H, Koller ET, Matsumoto T** 2000 Tumor necrosis factor-α represses androgen sensitivity in the LNCaP prostate cancer cell line. J Urol 164:800–805
63. **Shiota M, Izumi H, Onitsuka T, Miyamoto N, Kashiwagi E, Kidani A, Yokomizo A, Naito S, Kohno K** 2008 Twist promotes tumor cell growth through YB-1 expression. Cancer Res 68:98–105
64. **Shiota M, Izumi H, Onitsuka T, Miyamoto N, Kashiwagi E, Kidani A, Hirano G, Takahashi M, Naito S, Kohno K** 2008 Twist and p53 reciprocally regulate target genes via direct interaction. Oncogene 27:5543–5553
65. **Shiota M, Izumi H, Miyamoto N, Onitsuka T, Kashiwagi E, Kidani A, Hirano G, Takahashi M, Ono M, Kuwano M, Naito S, Sasaguri Y, Kohno K** 2008 Ets regulates peroxiredoxin1 and 5 expressions through their interaction with the high mobility group protein B1. Cancer Sci 99:1950–1959
66. **Shiota M, Izumi H, Tanimoto A, Takahashi M, Miyamoto N, Kashiwagi E, Kidani A, Hirano G, Masubuchi D, Fukunaka Y, Yasuniwa Y, Naito S, Nishizawa S, Sasaguri Y, Kohno K** 2009 Programmed cell death protein 4 down-regulates Y-box binding protein-1 expression via a direct interaction with Twist1 to suppress cancer cell growth. Cancer Res 69:3148–3156

Discrepancy Between Local and Central Pathological Review of Radical Prostatectomy Specimens

Kentaro Kuroiwa,* Taizo Shiraishi, Osamu Ogawa, Michiyuki Usami, Yoshihiko Hirao and Seiji Naito for the Clinicopathological Research Group for Localized Prostate Cancer Investigators

From the Department of Urology, Graduate School of Medical Sciences, Kyushu University, Fukuoka (KK, SN), Kyoto University Graduate School of Medicine, Kyoto (OO), Osaka Medical Center for Cancer and Cardiovascular Diseases, Osaka (MU), Nara Medical University, Kashihara (YH), and Department of Pathologic Oncology, Mie University Graduate School of Medicine, Tsu (TS), Japan

Abbreviations and Acronyms

CR = central review
CRPC = Clinicopathological Research Group for Localized Prostate Cancer
ECE = extracapsular extension
GS = Gleason score
ISUP = International Society of Urological Pathology
LNI = lymph node involvement
LR = local review
PSA = prostate specific antigen
PSM = positive surgical margin
RP = radical prostatectomy
SVI = seminal vesicle invasion

Submitted for publication June 29, 2009.
Presented at annual meeting of American Urological Association, Chicago, Illinois, April 25–30, 2009.
Study received institutional review board approval.

* Correspondence: Department of Urology, Graduate School of Medical Sciences, Kyushu University, 3-1-1 Maidashi, Higashi-ku, Fukuoka 812-8582 Japan (e-mail: humeiten@hotmail.com).

See Editorial on page 850.

Purpose: Pathological assessment of radical prostatectomy specimens has not been uniform among pathologists. We investigated interobserver variability of radical prostatectomy specimen reviews between local and central pathologists.
Materials and Methods: We collated data from 50 institutions on 2,015 patients with cT1c-3 prostate cancer who underwent radical prostatectomy between 1997 and 2005. All radical prostatectomy specimens were retrospectively reevaluated by a central uropathologist. Gleason score, extracapsular extension, seminal vesicle invasion, lymph node involvement, positive surgical margin, year of diagnosis and pathology volume were recorded.
Results: The exact concordance rate of Gleason score between local and central review was 54.8%, and under grading and over grading rates at local review were 25.9% and 19.2%, respectively. Spearman's rank correlation coefficient was 0.61 for local and central radical prostatectomy Gleason score. The exact concordance rate of Gleason score 8–10 at local review was significantly lower than that of Gleason score 5–6, 3 + 4 and 4 + 3 at local review ($p = 0.011$, <0.001 and 0.006). Exact concordance rates between local and central review for extracapsular extension, seminal vesicle invasion, lymph node involvement and positive surgical margin were 82.5%, 97.6%, 99.6% and 87.5%, respectively. High volume institutions and recently diagnosed cohorts showed significantly higher exact concordance rates between local and central review for radical prostatectomy Gleason score and other pathological features (all $p < 0.001$).
Conclusions: High volume institutions and recent series show higher concordance between local and central review of radical prostatectomy pathology. However, concordance for high grade Gleason score, extracapsular extension and surgical margin status remains poor. Radical prostatectomy specimens should be reevaluated in a multi-institutional study for more accurate pathological data.

Key Words: pathology, prostatic neoplasms, prostatectomy

PATHOLOGICAL features of radical prostatectomy specimens such as Gleason score, extracapsular extension, seminal vesicle invasion, lymph node involvement and positive surgical margin are crucial observations for physicians to assess the prognosis of each patient. Various nomograms predicting PSA relapse after RP have been constructed based on these pathological features combined with preoperative PSA.[1–3] Therefore, ideally these features should be diagnosed uniformly among pathologists. However, there is concern about

0022-5347/10/1833-0952/0
THE JOURNAL OF UROLOGY®

Vol. 183, 952-957, March 2010
Printed in U.S.A.
DOI:10.1016/j.juro.2009.11.024

interobserver variability for pathological features of RP specimens, which would affect prognostic accuracy.

Interobserver variability for biopsy GS among pathologists is well documented.[4–9] Biopsy GS assigned by pathologists at an academic center has been reported as better correlated with RP GS than that by pathologists at community centers.[4,9] However, to our knowledge interobserver variability for RP GS has not been investigated in a large contemporary RP series.

There are only a few studies of interobserver variability for other pathological features of RP specimens.[10–12] It was reported that the exact concordance between local and central review of RP specimens for ECE, SVI and PSM was 57.5%, 94.0% and 69.4%, respectively, in patients with pT3/PSM.[11] On the other hand, expert uropathologists indicated good concordance when evaluating ECE (91.2%, $\kappa = 0.63$) and PSM (90.4%, $\kappa = 0.74$).[12]

We investigated the interobserver variability between local and central pathologists for RP pathological features in a large RP series of 2,015 patients. Central review for GS was based on the 2005 ISUP consensus. In addition, we analyzed the impact of the date of diagnosis and pathology volume on interobserver variability.

MATERIALS AND METHODS

Patient Population

The CRPC disease registry collates data on clinically localized prostate cancer accrued from 108 academic and community practices throughout Japan. Between 1997 and 2005 patients with clinically localized (cT1c–3) prostate cancer who underwent RP were enrolled in the CRPC registry after obtaining institutional review board approval from each center.

Of these CRPC patients pathological slides of biopsy and prostatectomy specimens were available from 50 institutions in 2,015 patients with no preoperative therapy. In all patients preoperative diagnosis was made by systemic biopsy (6 or more cores). Preoperative serum PSA was known for all patients. Clinical stage was determined by digital rectal examination and was assigned according to the 2002 American Joint Committee on Cancer staging system.

Pathological Assessment

Prostatectomy specimens from the patients were processed by a whole mount technique after formalin fixation at each institution.[13] All pathological slides of biopsy specimens were reviewed by a uropathologist (TS). All pathological slides of RP specimens were reviewed by 1 uropathologist (KK) who has reviewed more than 5,000 RP cases. GS was assigned according to the 2005 ISUP consensus, and categorized into 5 groups of 2–4, 5–6, 3 + 4, 4 + 3 and 8–10.[14] Global GS that considered the entire tumor within the prostate as 1 lesion was recorded for RP specimens since the GS of each tumor was not available in the original reports for most patients. The exact concordance rate for categorized Gleason score between original (local) and central review was investigated. Tertiary Gleason pattern in RP specimens was not reflected as primary or secondary pattern on the final RP GS.

The presence of ECE, SVI, LNI and PSM was recorded for all RP specimens. ECE level was further categorized as focal ECE and established ECE.[15] ECE was assigned as positive when tumor cells existed beyond the confines of the prostate.[16] Direct contact between tumor cells and adipose tissue was not needed to assign ECE. The presence of tumor cells at the inked margin of resection was considered a PSM. For specimens that had not been inked before formalin fixation the presence of tumor cells at the noninked margin of resection was considered a PSM. SVI was assigned as positive when tumor cells had invaded into the muscular coat of the extraprostatic seminal vesicle. The positive to negative rate for ECE, SVI, LNI and PSM was defined as No. centrally negative cases in locally positive cases/No. locally positive cases. The negative to positive rate was defined conversely.

Data from original pathological reports for RP GS, ECE, SVI, LNI and PSM were available in 1,774, 1,630, 1,639, 1,914 and 1,579 patients, respectively. All data for ECE, SVI, LNI and PSM were available in 1,526 patients. For influence of date of diagnosis we compared patients diagnosed by local pathologists in 1997 to 2003 with those diagnosed in 2004 to 2005. For pathology volume we defined high volume institutions as those contributing 100 or more patients to the CRPC registry and low volume institutions as those contributing less than 100 patients.

Statistical Analysis

Spearman's rank correlation coefficient (r) on the relationship of RP GS was generated. Simple kappa statistics were used for concordance between local and central review in ECE, SVI, PNI and PSM. The chi-square test was used for comparison of the exact concordance rate between local and central review for each pathological feature. All p values are 2-sided and $p < 0.05$ considered significant.

RESULTS

Preoperative Characteristics

Median patient age was 66 years (range 42 to 84) and median PSA was 8.5 ng/ml (range 0.5 to 85.9). A total of 1,327 patients (65.9%) had cT1c disease. For biopsy specimens the distribution of central biopsy GS 2–4, 5–6, 3 + 4, 4 + 3 and 8–10 was 0.1% (2), 33.6% (677), 27.4% (552), 19.0% (382) and 20.0% (402), respectively (table 1).

Concordance for RP GS

Table 2 shows concordance for RP GS between local and central review. Spearman's rank correlation coefficient was 0.61 for local and central RP GS. Overall exact concordance between central and local review was 54.8%, and the under grading and over grading rate in local review was 25.9% and 19.2%, respectively. When GS 3 + 4 and 4 + 3 were combined the exact concordance rate was 66.0%. All 67 cases with local review GS 2–4 were upgraded to GS

Table 1. *Preoperative clinicopathological characteristics*

No. tumor stage (%):	
T1c	1,327 (65.9)
T2a	363 (18.0)
T2b	163 (8.1)
T2c	132 (6.6)
T3	30 (1.5)
No. ng/ml PSA distribution (%):	
4.0 or Less	152 (7.5)
4.1–10.0	1,135 (56.3)
10.1–20.0	543 (26.9)
20.1 or Greater	185 (9.2)

5–6 or more by central review and 36 (53.7%) were upgraded to GS greater than 7. At local review the exact concordance rate of GS 8–10 was significantly lower than that of GS 5–6, 3 + 4 and 4 + 3 ($p = 0.011$, <0.001 and 0.006, respectively). The distribution of GS 2–4, 5–6, 3 + 4, 4 + 3 and 8–10 changed from 3.8%, 32.0%, 33.0%, 15.7% and 15.6% on local review to 0.0%, 26.0%, 40.8%, 23.3% and 9.9%, respectively, on central review.

Concordance for ECE, SVI, LNI and PSM

Concordance for ECE, SVI, LNI and PSM is shown in table 3. Positive rate for each pathological feature was similar between local and central review. Exact concordance rates (κ) between local and central review for ECE, SVI, LNI and PSM were 82.5% (0.59), 97.6% (0.82), 99.6% (0.93) and 87.5% (0.73), respectively. Exact concordance for patients with no ECE, focal ECE and established ECE by central review was 85.8% (946 of 1,102), 57.9% (121 of 209) and 85.0% (271 of 319), respectively.

Of 528 patients with positive ECE on local review 157 had negative ECE on central review (positive to negative rate 29.7%), whereas 129 of 1,102 patients with negative ECE on local review had positive ECE on central review (negative to positive rate 11.7%). For SVI, LNI and PSM the positive to negative rate was 21.5%, 3.9% and 15.6%, and the negative to positive rate was 0.9%, 0.3% and 10.9%, respectively. Of 1,526 patients the complete concordance rate for ECE, SVI, LNI and PSM was 73.5% (1,121 of 1,526).

Pathology Volume

For RP GS we identified 1,063 patients from 10 high volume institutions and 711 from 37 low volume institutions. As shown in table 4 high volume institutions had significantly higher exact concordance between local and central review for RP GS than low volume institutions (60.9% vs 45.9%, $p < 0.001$). Of 1,526 patients with all data for ECE, SVI, LNI and PSM available 962 were from 10 high volume institutions and 564 were from 34 low volume institutions. High volume institutions also had significantly higher exact concordance rates for all of these features than low volume institutions (77.1% vs 67.2%, $p < 0.001$).

Date of Diagnosis

Overall patients originally diagnosed in 2004 to 2005 had a significantly higher exact concordance rate between local and central review than those diagnosed in 1997 to 2003 for RP GS (63.1% vs 48.2%, $p < 0.001$) and all other pathological features (78.6% vs 68.1%, $p < 0.001$, table 4). This improvement in pathological concordance in more recently diagnosed patients was observed at high and low volume institutions.

DISCUSSION

Pathological features on RP specimens are important for physicians to predict the prognosis of each patient.[1,2] Adjuvant radiotherapy or hormonal therapy might be selected for patients with adverse pathological features on RP specimens such as ECE, SVI, PSM and LNI, although RP may offer long-term survival even to such patients.[17–20] However, in reality pathological assessment is not performed uniformly among pathologists and interobserver variability does exist.

For biopsy specimens of prostate cancer interobserver variability for biopsy GS has been abundantly investigated.[4–9] Recent educational efforts by the pathology community might have improved biopsy GS concordance between community hospitals and academic centers.[4] The ISUP consensus also improved GS correlation between biopsy and RP spec-

Table 2. *Concordance for radical prostatectomy Gleason score between local and central review*

	No. CR RP GS*						
RP GS (No. LR)	5–6	3 + 4	4 + 3	8–10	% Exact Concordance	% Under Grading by LR vs CR	% Over Grading by LR vs CR
2–4 (67)	31	25	8	3	0	100	0.0
5–6 (567)	318	189	48	12	56.1	43.9	0.0
3+4 (585)	99	363	112	11	62.1	21.0	16.9
4+3 (279)	10	85	163	21	58.4	7.5	34.1
8–10 (276)	3	62	82	129	46.7	0.0	53.3
Overall (1,774)	461	724	413	176	54.8	25.9	19.2

* No cases of GS 2–4 on central review.

Table 3. *Concordance between local and central review*

LR	CR Pos	CR Neg	% Exact Concordance (κ value)	% Pos LR at RP	% Pos CR at RP	p Value	% Pos to Neg	% Neg to Pos
ECE:			82.5 (0.59)	32.4	30.7	0.291	29.7	11.7
Pos	371	157						
Neg	129	973						
SVI:			97.6 (0.82)	7.4	6.6	0.373	21.5	0.9
Pos	95	26						
Neg	13	1,505						
LNI:			99.6 (0.93)	2.7	2.8	0.767	3.9	0.3
Pos	49	2						
Neg	5	1,858						
PSM:			87.5 (0.73)	34.6	36.4	0.298	15.6	10.9
Pos	461	85						
Neg	113	920						

imens.[21] On the other hand, there are only a few reports regarding interobserver variability for pathological features on RP specimens.[10–12]

Significant discordance between general pathologists and uropathologists for RP GS has been reported in limited patients.[10] However, 22% of RP specimens were not processed by whole mount technique and detailed information for pathological assessment, such as categorization of GS and concordance in each GS, was not mentioned in that study. In our study using whole mount step sections and based on central review according to the ISUP consensus, the exact concordance rate between local and central review was 54.8%, and under grading or over grading in local pathology was observed in 25.9% and 19.2%, respectively. By central review the number of patients with RP GS 2–4, 5–6 and 8–10 decreased, and the number of those with RP GS 3 + 4 and 4 + 3 increased. Local pathologists in our study assigned RP GS 2–4 in 67 (3.8%) patients, whereas none did in central review. For biopsy specimens ISUP recommends that GS 2–4 should rarely, if ever, be diagnosed.[14] Because GS 2–4 was rarely assigned in contemporary RP series from academic centers, we would emphasize that GS 2–4 should seldom be assigned even in RP specimens.[4,21]

Table 4. *Impact of pathology volume and date of diagnosis on pathological concordance*

	No. RP GS Concordance (%)	No. ECE, SVI, LNI + PSM Concordance (%)
Pathology vol:		
Low	326/711 (45.9)	379/564 (67.2)
High	647/1,063 (60.9)	742/962 (77.1)
p Value	<0.001	<0.001
Date of diagnosis:		
1997–2003	473/981 (48.2)	511/750 (68.1)
2004–2005	500/793 (63.1)	610/776 (78.6)
p Value	<0.001	<0.001
Low/1997–2003	195/480 (40.6)	209/303 (62.8)
Low/2004–2005	131/231 (56.7)	170/231 (73.6)
p Value	<0.001	0.007
High/1997–2003	278/501 (55.5)	302/417 (72.4)
High/2004–2005	369/562 (65.7)	440/545 (80.7)
p Value	0.001	0.002

We also found poorer concordance between local and central review for high grade GS (8–10) compared with other GS (5–6, 3 + 4, 4 + 3). Of cases assigned as GS 8–10 by local review 53.3% were downgraded to 5–6, 3 + 4 or 4 + 3 by central review. This poor concordance in high grade GS may contribute to lower concordance between local and central review in our study compared with the previous study on biopsy GS that included only 32 high grade GS cases at local review (66.1% vs 76.5%).[4]

Unlike biopsy specimens with limited sample size, the discrepancy of GS in RP specimens among pathologists may reflect differences of interpretation itself for each Gleason pattern. We believe that this discrepancy can be effectively improved by educational effort as has been observed with biopsy specimens.[4] Indeed recently diagnosed RP specimens in our study showed higher GS concordance than those diagnosed earlier regardless of pathology volume. This improvement may be due to educational efforts by the pathology community as well as personal efforts of each pathologist even before the ISUP consensus. The ISUP consensus may result in further improvement for RP GS concordance between local and central review.

van der Kwast et al studied 552 RP specimens from multiple institutions, and observed poor concordance between local and central review for ECE (57.5%) and PSM (69.4%), and good concordance for SVI (94.0%).[11] Conversely good concordance was observed among 12 expert uropathologists for ECE (91.2%, $\kappa = 0.63$) and PSM (90.4%, $\kappa = 0.74$) in a small selected RP series.[12] We found excellent exact concordance for SVI (97.6%, $\kappa = 0.82$) and LNI (99.6%, $\kappa = 0.93$). The exact concordance rate in our study between local and central review for ECE (82.5%, $\kappa = 0.59$) and PSM (87.5%, $\kappa = 0.73$) was

better than that in a previous study comparing local and central pathologists (κ = 0.33 and 0.45).[11]

Although we should not simply compare κ values between studies because of the difference of data set, there may be some reasons for this difference. Since our study included more recently diagnosed patients, the effect of date of diagnosis as shown in our study may contribute to this higher concordance. Another contributing factor might be the fact that our patients underwent RP for cT1c–3 disease rather than more advanced disease (pT3 or PSM). The high κ values for ECE and PSM in our study as in a study with expert uropathologists (κ = 0.60 and 0.74) do not necessary mean that concordance in local and central pathologists is equivalent to that among expert uropathologists, because the study with expert uropathologists seems to include more difficult cases than our study.[12]

We found low concordance in patients with focal ECE at central review compared with those with established ECE (57.9% vs 85.0%). Since the prostate lacks a true histological capsule, and the boundaries between prostate and surrounding tissue are sometimes poorly defined especially with apical and anterior lesions, interobserver variability for ECE exists even among expert uropathologists.[12,22] ECE criteria for apical or anterior site remain to be established. Most cases in which definite judgment of ECE is difficult to make may have focal ECE.

We assigned PSM only when tumor cells touched the margin of resection. Most patients who were negative for PSM at local review and positive at central review were considered close to the margin by the central pathologist.

We also investigated the positive to negative and negative to positive rates for ECE, SVI, LNI and PSM. Although there were no differences regarding overall positive rates between local and central pathologists for each pathological feature, we found high positive to negative and negative to positive rates except for LNI. For SVI the positive to negative rate was 21.5% despite excellent overall concordance (97.6%).

It was previously reported that concordance between local and central review for ECE, SVI and PSM was essentially the same regardless of pathology volume.[11] We found that for GS and other pathological features local review at high volume institutions had higher concordance with central review than at low volume institutions. In high volume institutions there may be more communication between pathologists and urologists regarding pathological specimens, and pathologists may pay more attention to assessment for RP specimens. As in RP GS more recently diagnosed RP specimens in our study showed higher concordance for pathological features other than GS than those diagnosed at an earlier date in low and high volume institutions.

CONCLUSIONS

Although concordance between local and central pathologists was excellent for SVI and LNI, that for high grade GS, ECE and PSM was less satisfactory. This discrepancy may affect the outcomes of each pathological feature. High volume institutions showed higher concordance than low volume institutions. Although the concordance has recently improved, more educational and/or personal effort is warranted. For more precise pathological assessment we recommend central review for a study with RP specimens from multiple institutions.

REFERENCES

1. Kattan MW, Wheeler TM and Scardino PT: Postoperative nomogram for disease recurrence after radical prostatectomy for prostate cancer. J Clin Oncol 1999; **17:** 1499.
2. Stephenson AJ, Scardino PT, Eastham JA et al: Postoperative nomogram predicting the 10-year probability of prostate cancer recurrence after radical prostatectomy. J Clin Oncol 2005; **23:** 7005.
3. Walz J, Chun FK, Klein EA et al: Nomogram predicting the probability of early recurrence after radical prostatectomy for prostate cancer. J Urol 2009; **181:** 601.
4. Fine SW and Epstein JI: A contemporary study correlating prostate needle biopsy and radical prostatectomy Gleason score. J Urol 2008; **179:** 1335.
5. King CR: Patterns of prostate cancer biopsy grading: trends and clinical implications. Int J Cancer 2000; **90:** 305.
6. Lattouf JB and Saad F: Gleason score on biopsy: is it reliable for predicting the final grade on pathology? BJU Int 2002; **90:** 694.
7. Paulson DF: Impact of radical prostatectomy in the management of clinically localized disease. J Urol 1994; **152:** 1826.
8. San Francisco IF, DeWolf WC, Rosen S et al: Extended prostate needle biopsy improves concordance of Gleason grading between prostate needle biopsy and radical prostatectomy. J Urol 2003; **169:** 136.
9. Steinberg DM, Sauvageot J, Piantadosi S et al: Correlation of prostate needle biopsy and radical prostatectomy Gleason grade in academic and community settings. Am J Surg Pathol 1997; **21:** 566.
10. Ekici S, Ayhan A, Erkan I et al: The role of the pathologist in the evaluation of radical prostatectomy specimens. Scand J Urol Nephrol 2003; **37:** 387.
11. van der Kwast TH, Collette L, Van Poppel H et al: Impact of pathology review of stage and margin status of radical prostatectomy specimens (EORTC trial 22911). Virchows Arch 2006; **449:** 428.
12. Evans AJ, Henry PC, van der Kwast TH et al: Interobserver variability between expert urologic pathologists for extraprostatic extension and surgical margin status in radical prostatectomy specimens. Am J Surg Pathol 2008; **32:** 1503.

13. Montironi R, van der Kwast T, Boccon-Gibod L et al: Handling and pathology reporting of radical prostatectomy specimens. Eur Urol 2003; **44:** 626.

14. Epstein JI, Allsbrook WC Jr, Amin MB et al: The 2005 International Society of Urological Pathology (ISUP) Consensus Conference on Gleason Grading of Prostatic Carcinoma. Am J Surg Pathol 2005; **29:** 1228.

15. Wheeler TM, Dillioglugil O, Kattan MW et al: Clinical and pathological significance of the level and extent of capsular invasion in clinical stage T1-2 prostate cancer. Hum Pathol 1998; **29:** 856.

16. Srigley JR, Amin MB, Epstein JI et al: Updated protocol for the examination of specimens from patients with carcinomas of the prostate gland. Arch Pathol Lab Med 2006; **130:** 936.

17. Bolla M, van Poppel H, Collette L et al: Postoperative radiotherapy after radical prostatectomy: a randomised controlled trial (EORTC trial 22911). Lancet 2005; **366:** 572.

18. Messing EM, Manola J, Yao J et al: Immediate versus deferred androgen deprivation treatment in patients with node-positive prostate cancer after radical prostatectomy and pelvic lymphadenectomy. Lancet Oncol 2006; **7:** 472.

19. Thompson IM Jr, Tangen CM, Paradelo J et al: Adjuvant radiotherapy for pathologically advanced prostate cancer: a randomized clinical trial. JAMA 2006; **296:** 2329.

20. Boorjian SA, Thompson RH, Siddiqui S et al: Long-term outcome after radical prostatectomy for patients with lymph node positive prostate cancer in the prostate specific antigen era. J Urol 2007; **178:** 864.

21. Helpap B and Egevad L: The significance of modified Gleason grading of prostatic carcinoma in biopsy and radical prostatectomy specimens. Virchows Arch 2006; **449:** 622.

22. Ayala AG, Ro JY, Babaian R et al: The prostatic capsule: does it exist? Its importance in the staging and treatment of prostatic carcinoma. Am J Surg Pathol 1989; **13:** 21.

Published OnlineFirst February 9, 2010; DOI:10.1158/0008-5472.CAN-09-2984

AACR

Cancer Research

Identification of EP4 as a Potential Target for the Treatment of Castration-Resistant Prostate Cancer Using a Novel Xenograft Model

Naoki Terada, Yosuke Shimizu, Tomomi Kamba, et al.

Cancer Res 2010;70:1606-1615. Published OnlineFirst February 9, 2010.

Published OnlineFirst February 9, 2010; DOI:10.1158/0008-5472.CAN-09-2984

Therapeutics, Targets, and Chemical Biology

Cancer Research

Identification of EP4 as a Potential Target for the Treatment of Castration-Resistant Prostate Cancer Using a Novel Xenograft Model

Naoki Terada[1], Yosuke Shimizu[1], Tomomi Kamba[1], Takahiro Inoue[1], Atsushi Maeno[1], Takashi Kobayashi[1], Eijiro Nakamura[1,6], Toshiyuki Kamoto[1,7], Toshiya Kanaji[8], Takayuki Maruyama[8], Yoshiki Mikami[2], Yoshinobu Toda[3], Toshiyuki Matsuoka[4], Yasushi Okuno[5], Gozoh Tsujimoto[5], Shuh Narumiya[4], and Osamu Ogawa[1]

Abstract

More effective therapeutic approaches for castration-resistant prostate cancer (CRPC) are urgently needed, thus reinforcing the need to understand how prostate tumors progress to castration resistance. We have established a novel mouse xenograft model of prostate cancer, KUCaP-2, which expresses the wild-type androgen receptor (AR) and which produces the prostate-specific antigen (PSA). In this model, tumors regress soon after castration, but then reproducibly restore their ability to proliferate after 1 to 2 months without AR mutation, mimicking the clinical behavior of CRPC. In the present study, we used this model to identify novel therapeutic targets for CRPC. Evaluating tumor tissues at various stages by gene expression profiling, we discovered that the prostaglandin E receptor EP4 subtype (EP4) was significantly upregulated during progression to castration resistance. Immunohistochemical results of human prostate cancer tissues confirmed that EP4 expression was higher in CRPC compared with hormone-naïve prostate cancer. Ectopic overexpression of EP4 in LNCaP cells (LNCaP-EP4 cells) drove proliferation and PSA production in the absence of androgen supplementation *in vitro* and *in vivo*. Androgen-independent proliferation of LNCaP-EP4 cells was suppressed when AR expression was attenuated by RNA interference. Treatment of LNCaP-EP4 cells with a specific EP4 antagonist, ONO-AE3-208, decreased intracellular cyclic AMP levels, suppressed PSA production *in vitro*, and inhibited castration-resistant growth of LNCaP-EP4 or KUCaP-2 tumors *in vivo*. Our findings reveal that EP4 overexpression, via AR activation, supports an important mechanism for castration-resistant progression of prostate cancer. Furthermore, they prompt further evaluation of EP4 antagonists as a novel therapeutic modality to treat CRPC. *Cancer Res; 70(4); 1606–15. ©2010 AACR.*

Introduction

Prostate cancer is one of the most frequently diagnosed cancers in the Western world (1). Because prostate cancer development is initially dependent on androgens, medical or surgical castration is the mainstay therapy for patients with advanced prostate cancer. However, most patients ultimately relapse after a period of initial response to this therapy, progressing to castration-resistant prostate cancer (CRPC). Effective therapeutic approaches for CRPC are extremely limited. Treatment with docetaxel was established as a new standard of care for CRPC patients (2). However, it is not curative, and optimal timing of administration remains controversial. Consequently, it is highly desirable to explore new therapeutic strategies based on detailed molecular mechanisms for the development of castration resistance in prostate cancer.

The generation of suitable *in vivo* models is critical to better understand the processes associated with the development and progression of prostate cancer. We have previously reported a novel prostate cancer xenograft model named KUCaP-1 (previously referred to as KUCaP; ref. 3). KUCaP-1 tumors harbor the W741C mutant androgen receptor (AR), regress soon after castration in mice, and do not regrow with long-term follow-up (4). We have now established another novel xenograft model named KUCaP-2 using locally recurrent CRPC specimens derived from a different patient. The KUCaP-2 tumors harbor wild-type AR, regress soon after castration, and restore their ability to proliferate after 1 to 2 months without AR mutation. As the sequential changes of the xenograft resemble the clinical behavior of prostate cancer, this model may provide an excellent system to

Authors' Affiliations: [1]Department of Urology, Kyoto University Graduate School of Medicine; [2]Department of Diagnostic Pathology, Kyoto University Hospital; [3]Anatomical Center, Kyoto University Graduate School of Medicine; [4]Department of Pharmacology, Faculty of Medicine, Kyoto University; [5]Department of Genomic Drug Discovery Science, Kyoto University Graduate School of Pharmaceutical Sciences, Kyoto, Japan; [6]Department of Medical Oncology, Dana-Farber Cancer Institute, Boston, Massachusetts; [7]Department of Urology, Miyazaki University, Miyazaki, Japan; and [8]Development Research Laboratories, Research Headquarters, Ono Pharmaceutical Co., Ltd., Osaka, Japan

Corresponding Author: Osamu Ogawa, Department of Urology, Kyoto University Graduate School of Medicine, 54, Shogoinkawahara-cho, Sakyo-ku, Kyoto 606-8507, Japan. Phone: 81-75-751-3325; Fax: 81-75-761-3441; E-mail: ogawao@kuhp.kyoto-u.ac.jp.

doi: 10.1158/0008-5472.CAN-09-2984

Published OnlineFirst February 9, 2010; DOI:10.1158/0008-5472.CAN-09-2984

study the mechanisms associated with castration-resistant progression of prostate cancer and to evaluate new treatment modalities for CRPC.

In KUCaP-2, prostaglandin E receptor EP4 subtype (EP4) expression significantly increased with the development of castration resistance. We explored the function of EP4 in prostate cancer cells as a potential target for the treatment of CRPC.

Materials and Methods

Generation of xenograft model. Clinical materials were used after informed consent was obtained, according to protocols approved by the institutional review board at Kyoto University Hospital. All experiments involving laboratory animals were done in accordance with the Guideline for Animal Experiments of Kyoto University. Local recurrent tumors after radical prostatectomy were resected trans-urethrally, minced into 20 to 30 mm^3 tumor bits, and transplanted s.c. into 5-wk-old male nude mice (Charles River Japan) with 50 μL of Matrigel (Becton Dickinson) injected around the implant. The KUCaP-2 xenograft was established ~10 mo after the first inoculation. The xenograft tumors were extracted and transplanted to several mice without Matrigel. Ninety percent of the tumor was serially transplantable.

Sequence analysis. Genomic DNA from the xenograft tissue was extracted and all of the exons of the *AR* gene were sequenced as previously reported (3).

Tissue sampling and DNA microarray analysis. The mice bearing KUCaP-2 tumors were castrated and the sequential changes in tumor volume were analyzed as previously reported (3). Serum samples were obtained at sacrifice to measure prostate-specific antigen (PSA) values. Xenograft tissues of KUCaP-2 were collected during various stages and total RNA was isolated and purified using the RNeasy Mini Kit (Qiagen). Changes in gene expression were analyzed using DNA microarray analysis with an Affymetrix Human Genome U133 Plus2.0.

Real-time PCR. cDNA was synthesized from total RNA using a First-Strand cDNA Synthesis Kit (Amersham Pharmacia Biotech). Real-time PCR was performed using SYBR green PCR Master Mix (Applied Biosystems) and monitored using GeneAmp 5700 (Applied Biosystems) in triplicate. The thermal cycling conditions were 95°C for 15 s, 60°C for 30 s, and 72°C for 30 s. The values were normalized to the levels of amplified glyceraldehyde-3-phosphate dehydrogenase (GAPDH). The sequences of primers were as follows: EP4, 5′-GGAAATGACCAGGCCAAGAC-3′ (sense) and 5′-CAACCCTGGACCTCACACCTA-3′ (antisense); PSA, 5′-GGAAATGACCAGGCCAAGAC-3′ (sense) and 5′-CAACCCTGGACCTCACACCTA-3′ (antisense); AR, 5′-CTTCACCAATGTCAACTCCA-3′ (sense) and 5′-TCATTCGGACACACTGGCTG-3′ (antisense); and GAPDH, 5′-GAATATAATCCCAAGCGGTTTG-3′ (sense) and 5′-ACTTCACATCACAGCTCCCC-3′ (antisense).

Antibodies and reagents. Anti-AR (C-19: sc-815) and anti-PSA (C-19: sc7638) antibodies were obtained from Santa Cruz Biotechnology. Anti-β-actin antibody (AC-15: ab6276) was purchased from Abcam. Anti-EP4 antibody (COOH terminus: 101775) for Western blotting was obtained from Cayman Chemical and anti-EP4 antibody (N terminus: LS-A3898) for immunohistochemistry was obtained from MBL International. The EP4-specific antagonist ONO-AE3-208 was provided by Ono Pharmaceutical Co. (5). 5α-Dihydrotestosterone was purchased from Sigma. Forskolin, an activator of adenylate cyclase, and dibutyryl cyclic AMP (dbcAMP), a cAMP analogue, were purchased from Nacalai Tesque. H-89, a cAMP-dependent protein kinase (PKA) inhibitor, was obtained from Biomol International. An expression vector, pcDNA3.1-EP4, was constructed by inserting the cDNA of human EP4, digested from a cloning vector, pBluescript-EP4 (6), into *Hin*dIII-*Bam*HI sites of pcDNA3.1(−). Vectors were transfected into the cells using Lipofectamine 2000 reagent (Invitrogen) and transfectants were selected by geneticin (Nacalai Tesque).

Western blotting and immunohistochemistry. Western blotting was performed with each primary antibody (AR, 1:400; PSA, 1:400; EP4 1:700; β-actin, 1:5,000) as previously reported (7). Immunohistochemistry was performed by standard indirect immunoperoxidase procedures using each primary antibody (AR, 1:100; PSA, 1:100; EP4 1:400), and the reaction was enhanced by microwave only in EP4 immunohistochemistry. Hormone-naïve prostate cancer (HNPC) tissues were derived from radical prostatectomy specimens of localized prostate cancer patients as tissue microarrays constructed as previously reported (8, 9). CRPC tissue samples were local tumors obtained from patients undergoing transurethral resection or autopsy. The expression intensity was graded as none, weak, moderate, and strong by a clinical pathologist (Y.M.) who was blind to the clinicopathologic data. The grading was determined based on the intensity of staining for at least 20% of the cancer cells.

Cell culture. The prostate cancer cell lines LNCaP, DU145, and PC3 were obtained from the American Type Culture Collection, passaged for fewer than 6 mo after resuscitation. The cells were routinely cultured in RPMI 1640 (Invitrogen) supplemented with 10% fetal bovine serum. For androgen-depleted conditions, cells were cultured in phenol red–free RPMI 1640 (Invitrogen) supplemented with 10% charcoal-stripped fetal bovine serum (CSFBS; Hyclone). To analyze the cell proliferation *in vitro*, 1.0×10^5 cells per well were seeded into six-well plates and grown for indicated days, and then cell numbers were counted in triplicate by a hemocytometer. For the assessment of *in vivo* tumor growth, 0.5×10^7 to 1.0×10^7 cells were inoculated with 100 μL Matrigel in the flank region of 5-wk-old male nude mice, and tumor volumes were measured once weekly.

RNA interference. AR knockdown was performed using stealth RNAi [stAR(1);HSS100620 and stAR(2);HSS100619] compared with control nonspecific stealth RNAi (stCtr;12935-400) purchased from Invitrogen. Cells were seeded at 5.0×10^5 per well in six-well plates and incubated for 24 h. Each 160 pmol of stealth RNAi was transfected using Lipofectamine 2000 reagent.

Luciferase assay. Cells were seeded at 1.5×10^5 per well in 24-well plates and were transiently cotransfected with 250 ng

Published OnlineFirst February 9, 2010; DOI:10.1158/0008-5472.CAN-09-2984

of pcDNA3.1-EP4, 250 ng of pGL3-PSAp-Luc, and 5 ng of pTK-RL using Lipofectamine 2000 reagent. After 24 h of incubation, the medium was changed to create androgen-depleted conditions and the cells were incubated again for 24 h. The luciferase activity of the cell lysate was measured using the Dual-Luciferase Reporter Assay System (Promega) with a luminometer (MicroLumat Plus LB96V, Berthold Technologies) in triplicate.

cAMP assay. Cells were seeded at 1.0×10^5 per well in 96-well plates and incubated for 24 h. Cells were washed once with PBS and cultured for 1 h in androgen-depleted conditions. The intracellular cAMP concentrations were assayed using the cAMP-EIA kit (RPN225; Amersham-Pharmacia Biotech) in duplicate. ONO-AE3-208 was added 10 min before the assay.

Statistical analysis. The data were expressed as mean ± SD and their statistically significant differences were determined by one-way ANOVA. Age, serum PSA levels, Gleason sums, and tumor volumes were compared by the Mann-Whitney *U* test, and EP4 staining levels were compared by the χ^2 test. Statistical analyses were all performed using SPSS software.

Results

KUCaP-2 is an androgen-dependent prostate cancer xenograft harboring wild-type AR, producing PSA, and developing castration resistance without AR mutation. Tumor tissues used for the establishment of KUCaP-2 were histologically diagnosed as prostate cancer based on positive AR and PSA immunohistochemistry staining (Fig. 1A). Western blotting analysis revealed that KUCaP-2 cells expressed AR and PSA (Fig. 1B). In mice, the KUCaP-2 tumor regressed soon after castration and reproducibly regrew after 1 to 2 months. Sequence analysis of *AR* in KUCaP-2 tumors before and after castration showed no *AR* mutation.

Xenograft tissues of KUCaP-2 were transplanted into 12 mice and collected during androgen-dependent growth (AD), castration-induced regression nadir (ND), and castration-resistant regrowth (CR) stages (n = 4, each; Fig. 1C). The tumor volumes were 3,012 ± 467, 562 ± 208, and 1,962 ± 560 mm^3, and the median PSA values of the mice were 166.0, 4.0, and 50.9 ng/mL for the AD, ND, and CR stages, respectively. There was no histologic difference among KUCaP-2 tumors of each stage (Fig. 1D, a–c). The nuclear expression levels decreased from the AD stage to the ND stage, indicating that the depletion of circulating androgen suppressed nuclear expression of AR in KUCaP-2 tumors at the ND stage. Nuclear expression recovered at the CR stage to levels similar to those at the AD stage (Fig. 1D, d–f).

EP4 expression was upregulated with the progression of castration resistance in KUCaP-2 tumors. To elucidate the mechanisms responsible for the development of castration resistance, we evaluated the gene expression profiles of tumors at each stage using DNA microarray analyses. In total, for 2,476 genes, there was a significant difference ($P < 0.05$) in expression between at least two stages. The k-means clustering (k = 10) of these genes was performed to select candidate genes (Fig. 2A). Previous reports on DNA microarray analysis in several different xenograft models showed that *AR* was the only gene consistently upregulated during castration-resistant progression (10). In our study, *AR* expression slightly increased from the AD stage to the ND stage (ratio = 2.7, P = 0.006), with no difference between the ND and CR stages (ratio = 1.1, P = 0.280). The *PSA* expression of tumors slightly and not significantly decreased from the AD stage to the ND stage (ratio = 0.6, P = 0.138) and recovered at the CR stage. To find genes associated with castration resistance, we explored genes in the cluster whose expression levels were low in both the AD and ND stages but high in the CR stage. Among 111 genes in this cluster, the CR/ND ratio of *EP4* expression was the highest (ratio = 15.7, P = 0.029; Table 1). These results were validated by real-time PCR analysis (Fig. 2B). Moreover, *EP4* expression was higher in the androgen-independent cell lines (DU145, PC3) compared with an androgen-dependent cell line (LNCaP; data not shown), consistent to other reports (11–13).

EP4 expression was higher in clinical CRPC than in HNPC. EP4 was mainly expressed in cellular membranes or in the cytoplasm of KUCaP-2 tumor cells, with more expression at the CR stage compared with the AD stage (Fig. 2C, a,b). Using KUCaP-2 samples from CR and AD stages as positive and negative controls, respectively, staining intensity of EP4 in clinical materials from 27 HNPC and 31 CRPC patients was graded (Fig. 2C, c–f). The characteristics of these patients were shown in Table 2. All the CRPC patients had PSA relapse. The serum PSA level and the Gleason sum were higher in CRPC than in HNPC. The EP4 expression level was significantly higher in CRPC than in HNPC (P = 0.0001).

EP4 overexpression induced castration-resistant progression of LNCaP cells through AR activation. We examined whether EP4 overexpression induced castration-resistant progression using LNCaP. LNCaP cells were stably transfected with pcDNA3.1-EP4, and two monoclonal EP4-overexpressing LNCaP clones were established and named LNCaP-EP4(A) and LNCaP-EP4(B). The EP4 signal activates adenylate cyclase, which results in acceleration of the production of cAMP (14). The intracellular cAMP concentrations, PSA expression levels, and cell proliferation ratio of LNCaP-EP4 without androgen were higher compared with those in vector alone–transfected LNCaP (LNCaP-mock) cells, indicating that overexpressed EP4 protein activated adenylate cyclase and induced PSA expression and cell proliferation without androgen (Fig. 3A).

To examine whether AR activation is associated with androgen-independent PSA expression and cell proliferation in LNCaP-EP4, AR expression was attenuated using a stealth RNAi system. PSA expression without androgen was suppressed more significantly by the attenuation of AR in LNCaP-EP4 cells than in LNCaP-mock cells. Further, the suppression of androgen-independent cell proliferation was statistically significant in LNCaP-EP4 cells, but not in LNCaP-mock cells, indicating that AR activation was associated with androgen independence of LNCaP-EP4 cells (Fig. 3B). We examined the effect of EP4 on AR activation using